NATIONAL TECHNICAL UNIVERSITY OF ATHENS

School of Civil Engineering

Laboratory for Earthquake Engineering

Seismic Response Assessment of Rigid and Flexible Rocking Bodies using Simple Finite Element Models

Spyridon G. Diamantopoulos

A dissertation submitted in partial satisfaction of the

requirements for the degree

MSc in Analysis & Design of Earthquake Resistant Structures

Supervisor:
Dr. Michalis Fragiadakis
Assistant Professor NTUA

Athens, March 2017

Research topics*:* *Earthquake Engineering, Finite Element Modeling*

Key words: *rocking structures, rigid blocks, flexible blocks, seismic response, fem modeling, non-linear dynamic analyses*

Spyridon G. Diamantopoulos, Dipl (School of Civil Engineering, NTUA, 2013)

Dr. Michalis Fragiadakis, Assistant Professor NTUA

Seismic Response Assessment of Rigid and Flexible Rocking Bodies using Simple Finite Element Models

MSc in Analysis & Design of Earthquake Resistant Structures

Master's Dissertation

Laboratory for Earthquake Engineering, School of Civil Engineering, National Technical University of Athens, Greece, 2017.

Preface

This master's dissertation was started, conducted and written at the Laboratory for Earthquake Engineering of the School of Civil Engineering, at the National Technical University of Athens (NTUA). It is a result of nearly a year's work and marks the end of my Master of Science studies in Structural Engineering, emphasizing on Finite Element Modeling (FEM), non-linear dynamic analyses and the seismic response of Rocking Bodies. From the beginning until its very end, the dissertation was supervised closely, by the Assistant Professor of the Laboratory for Earthquake Engineering of NTUA, Dr. Michalis Fragiadakis.

Acknowledgments

The last step for obtaining the MSc degree in Structural Engineering at the National Technical University of Athens is this dissertation. I would like to express my deepest gratitude to my supervisor Michalis Fragiadakis, for giving me the opportunity to work with him on such an interesting topic. Our collaboration was exceptional and I can only feel grateful and proud from the whole experience all this months. I would also like to express my appreciation for his support on the decisions I made during this time concerning my future and state that his insight, guidance and patience prepared me for the next step. The most significant is the trust of my supervisor to continue our collaboration giving me the opportunity to persevere in my studies at the National Technical University of Athens as a researcher. This fact gives me the strength to continue and I wish to reward him.

Special thanks to Zmpenti for encouraging and supporting me in every decision relevant to my career and my targets.

Last but not least, I would like to thank my family (George, Maria, Pantelis, Ioannis) and friends for enduring me all these years of my academic career, commiserating my concerns and supporting me every day of my life.

Table of Contents

Abstract

This master's dissertation examines different approaches for modeling the seismic response of blocks that are either rigid or flexible. All models examined are formed with the aid of simple beam-column elements and thus can be implemented with any finite element (FE) software. We first study blocks that can be considered as rigid and we compare our findings with results obtained after solving directly the block's equation of motion as derived by Housner's theory. We compare three FE models which are based on single-degree-of-freedom oscillators (SDOF). The models include a rigid column connected to a zero-length non-linear elastic rotation spring with a negative-stiffness moment-rotation relationship. Both continuous and event-based damping is considered. The proposed models are compared using simple wavelets and also natural ground motion records. In the case of ground motion records, event-based damping produced superior results compared to the continuous case, since energy dissipation in rocking blocks takes place instantaneously at every impact. The proposed FE approach is expanded to the case of flexible blocks offering a modeling that is considerably simpler than other approaches in the literature and is able to provide very accurate solutions within a fraction of the CPU time required if the block was modeled with a full mesh of quadrilateral elements.

Extended Summary (in Greek)

Ο σεισμός είναι ένα φαινόμενο το οποίο εκδηλώνεται συνήθως χωρίς προειδοποίηση, δεν μπορεί να αποτραπεί και παρά τη μικρή χρονική διάρκειά του, μπορεί να προκαλέσει μεγάλες ζημιές στις υποδομές με επακόλουθα τραυματισμούς, απώλειες ανθρώπινων ζωών, ρευστοποίηση εδαφών, καταπτώσεις βράχων και δημιουργία θαλάσσιων κυμάτων (τσουνάμι). Για το λόγο αυτό πλήθος ερευνών διεξάγονται προκειμένου να προσεγγιστεί η απόκριση των κατασκευών σε δυναμικές φορτίσεις.

Δομικά συστήματα ή αντικείμενα στα οποία η σημαντική παράμετρος της απόκρισης υπό δυναμικές φορτίσεις δεν είναι η παραμόρφωση του υλικού αλλά η μετακίνηση της κατασκευής είναι αυτά που εξετάζονται στην παρούσα εργασία. Τέτοια δομικά συστήματα (αρχαία μνημεία, μουσειακά εκθέματα, έπιπλα κ.α.) από «ισχυρά» υλικά θεωρούνται άκαμπτα ή σχεδόν άκαμπτα και εδράζονται ελεύθερα στη βάση τους. Συνήθως, η κινήση τέτοιων σωμάτων είτε στο επίπεδο είτε στο χώρο όταν αυτά υποβληθούν σε εξωτερική διέγερση ισοδυναμεί με κίνηση απολύτως στερεού σώματος. Στην περίπτωση, όμως, σωμάτων που δεν μπορούν να θεωρηθούν απόλυτα άκαμπτα και οι μετακινήσεις δεν οφείλονται αποκλειστικά σε κίνηση στερεού σώματος αλλά και σε μετακινήσεις λόγω κάμψης τα πράγματα γίνονται περίπλοκα. Ως αποτέλεσμα, η συμπεριφορά τέτοιων αντικειμένων, σωμάτων ή δομικών στοιχείων που εδράζονται ελεύθερα και που πολλές φορές αποτελούν πολιτισμική κληρονομιά χρήζει αντικείμενο μελέτης. Σκοπός της εργασίας είναι η μελέτη της σεισμικής απόκρισης ελεύθερα εδραζομένων σωμάτων είτε άκαμπτων είτε εύκαμπτων σε σχεδόν άκαμπτη επιφάνεια και στόχος η δημιουργία μοντέλων και η προσέγγιση της συμπεριφοράς κάτω από σεισμικές διεγέρσεις.

Στο κεφάλαιο 1 παρουσιάζονται οι διαφορετικοί τρόποι απόκρισης ενός σώματος ελεύθερα εδραζόμενου υπό μια σεισμική διέγερση. Αποδεικνύεται ο λόγος για τον οποίο η ολίσθηση αμελείται στην παρούσα εργασία, οι δυο διαφορετικοί τρόποι ανατροπής ενός σώματος καθώς και ο ορισμός της λικνιστικής συμπεριφοράς που είναι και το αντικείμενο της εργασίας.

Το κεφάλαιο 2 περιλαμβάνει την αναγνώριση του προβλήματος του λικνισμού άκαμπτων σωμάτων ελεύθερα εδραζόμενων σε άκαμπτη επιφάνεια, την επίλυση της εξίσωσης κίνησης, τη γραμμικοποίηση της εξίσωσης κίνησης και τη δυνατότητα επίλυσης αυτής με τη βοήθεια ενός solver που διατείθεται στη MATLAB. Στόχος ήταν η δημιουργία μοντέλων που θα προσεγγίζουν τη συμπεριφορά αυτή χωρίς τη μοντελοποίηση του φορέα με τετρακομβικά πεπερασμένα στοιχεία πράγμα που οδηγεί σε χρονοβόρες αναλύσεις. Για το σκοπό αυτό παρουσιάζονται στο κεφάλαιο 2 τα μοντέλα που δημιουργήθηκαν στο λογισμικό OpenSees και η απόκρισή τους συγκρίνεται με την απόκριση από την επίλυση της εξίσωσης κίνησης. Η προσομοίωση έγινε με 4 διαφορετικούς ταλαντωτές, χρησιμοποιήθηκαν beam-column elements συνδεόμενα στη βάση με ένα στροφικό ελατήριο για το οποίο εξαετάστηκαν δύο διαφορετικοί νόμοι ροπής-στροφής. Για την επιβεβαίωση των αποτελεσμάτων πραγματοποιήθηκαν δυναμικές αναλύσεις με διάφορους παλμούς και πραγματικές σεισμικές καταγραφές, έγινε σύγκριση των καμπυλών Pushover, των μετακινήσεων και των ροπών ανατροπής.

Στο κεφάλαιο 3 έγινε μια διερεύνηση σχετική με την απώλεια ενέργειας που συμβαίνει κατά την κίνηση ενός λικνιζόμενου δομικού συστήματος. Έχουν προταθεί κατά καιρούς διαφορετικοί τρόποι προσέγγισης του θέματος οι οποίοι εξετάστηκαν και αναλύθηκαν. Αρχικά, η απώλεια ενέργειας προσεγγίστηκε με έναν αποσβεστήρα τοποθετημένο στη βάση του στύλου και προσφέροντας συνεχή απόσβεση. Στη συνέχεια εξετάστηκε η περίπτωση της αριθμητικής απόσβεσης (numerical damping) και της προσομοίωσης της απόσβεσης σύμφωνα με τον κανονισμό FEMA-356. Αυτό που αξίζει να σημειωθεί είναι το γεγονός πως απώλεια ενέργειας σε τέτοια δομικά συστήματα συμβαίνει μόνο κατά τις στιγμές της κρούσης του σώματος στην επιφάνεια. Για το λόγο αυτό, αν και από τις προηγούμενες προσομοιώσεις προκύπτουν ικανοποιητικά αποτελέσματα, αναζητήθηκε ένας τρόπος στιγμιαίας απόσβεσης τη στιγμή της κρούσης. Έτσι τροποποιήθηκαν τα απλοποιητικά μοντέλα πεπερασμένων στοιχείων του κεφαλαίου 2, συσχετίζοντας τις γωνιακές ταχύτητες των κόμβων με το συντελεστή αποκατάστασης κάθε στιγμή στην οποία λαμβάνει χώρα μια κρούση (event-based damping). Πλήθος αναλύσεων με παλμούς και πραγματικές καταγραφές επιβεβαιώνουν την ορθότητα των αποτελεσμάτων.

Στο κεφάλαιο 4 στόχος ήταν ο έλεγχος του τελευταίου μοντέλου στην περίπτωση των εύκαμπτων σωμάτων και ο υπολογισμός της απόκρισης συμπεριλαμβανομένων των

καμπτικών μετακινήσεων. Επιλύθηκε ένα συγκεκριμένο σώμα στο πρόγραμμα Abaqus υπό παλμική και σεισμική διέγερση για την επιβεβαίωση της ορθότητας των αποτελεσμάτων που προκύπτουν από το μοντέλο 4 ενώ στη συνέχεια έγινε μια παραμετρική ανάλυση όπου και παρουσιάζονται οι διαφορές στην απόκριση μεταξύ ενός εύκαμπτου και άκαμπτου λικνιζόμενου σώματος.

Η παρούσα εργασία αποτελεί ένα τρόπο εκτίμησης και προσέγγισης της σεισμικής συμπεριφοράς σωμάτων που υποβάλλονται σε λικνιστική κίνηση μέσω απλών μοντέλων ενώ οδήγησε σε κρίσιμα συμπεράσματα σχετικά με την κατανοήση ενός τόσο ενδιαφέροντος και ταυτόχρονα περίπλοκου θέματος. Τα συμπεράσματα παρατίθενται στο κεφάλαιο 5 ενώ προτείνονται ιδέες για μελλοντική έρευνα.

Το κεφάλαιο 6 περιλαμβάνει βιβλιογραφικές αναφορές που αποτελούν ένα καλό οδηγό για τη μελέτη παρόμοιων ερευνητικών θεμάτων.

List of Figures

1. Introduction

1.1. Presentation of the problem

Reconnaissance reports following strong earthquakes substantiate that a solitary free-standing solid body subjected to a seismic excitation of the base can uplift, slide, rock or overturn. The need to understand and predict these failures in association with the temptation to estimate levels of ground motion by examining whether slender structures have overturned or survived the earthquakes, has motivated a number of studies on the response of blocks.

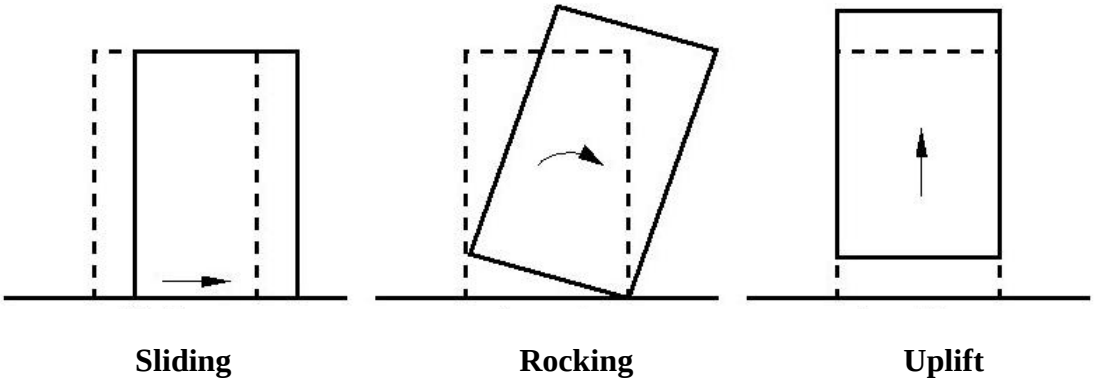

Figure 1: Seismic Response of a solitary free-standing solid body under a seismic excitation.

The phenomenon of the partial uplift of a structure from its foundation and its oscillation when the center of rotation changes simultaneously from one point of reference to another is known in the literature as rocking and it is often observed during seismic excitations. The study of rocking motion in structures is crucial because as it was indicated by many researchers slender structures may rock on their foundation, a phenomenon which can be devastating in some cases. Rocking motion introduces a highly nonlinear mechanical problem due to the fact that it involves a wide range of nonlinear physical phenomena, such as impact, contact, uplift and sliding. Therefore, the mathematical formulation and solution of the full rocking problem is a rather difficult task. For this reason, numerical modeling through nonlinear finite element analysis is one of the most suitable tools for a wide range of dynamic rocking problems, as it is able to provide accurate prediction of the rocking motion. However,

the utilization of nonlinear finite element analysis requires special attention and validation of the obtained results by means of comparison with experimental or analytical solutions. The purpose of this master's dissertation is to approach the seismic response of rocking blocks subjected to pulses-like ground excitation or real records with the Finite Element Method taking into account the nonlinear physical phenomena and the difficulties of an analytical formulation and solution.

1.2. Sliding of Solitary Blocks – Coefficient of friction

During the dynamic movement of a free-standing solid body due to the base excitation a nonlinear phenomenon which may take place is sliding. A body slides if it can't follow the ground motion. The friction in the interface between the base and the body has a direction parallel to the interface and is produced by the relative displacement of the two surfaces in contact and does not depend on their sliding velocities. If the horizontal force exceeds the static force of friction (which is a boundary value) then the body is sliding. The ratio of the static force of friction to the vertical base resistance is called static coefficient of friction:

$$\mu_{st} = \frac{T_{st}}{N} \tag{1.1}$$

During the sliding the body continues to exist forces of friction. The requirement for continuation of sliding with fixed velocity is a horizontal force called sliding force of friction and is constant during the sliding of the body. The ratio of the sliding force of friction to the vertical base resistance is called sliding coefficient of friction:

$$\mu_{tot} = \frac{T_{tot}}{N} \tag{1.2}$$

and it is generally accepted that $\mu_{tot} < \mu_{st}$. The static coefficient of friction and the sliding coefficient of friction is independent of the body mass and the area of the contact surface and depends only from the kind of the contact surfaces.

Assuming that $\ddot{V}$ and $\ddot{U}$ are the vertical and horizontal base accelerations respectively, X and Y are the horizontal and vertical displacements, $\dot{X}$ and $\dot{Y}$ are the velocities and $\ddot{X}$ and $\ddot{Y}$ are the horizontal and vertical accelerations respectively of the body.

According to the principle of D' Alembert the equations of motion of the body will be:

$$m\ddot{X} = T \tag{1.3}$$

$$m\ddot{Y} = N - mg \tag{1.4}$$

where m is the body mass. Modifying the above equations we have as a result:

$$T = m\ddot{U} \tag{1.5}$$

$$N = mg\left(1+\frac{\ddot{V}}{g}\right) \tag{1.6}$$

In order to slide the free-standing solitary body the inertial force must be at least the same with the static force of friction, namely:

$$m\ddot{X} \geq T_{st} \tag{1.7}$$

Taking into account all the above is arising:

$$\begin{aligned} &m\ddot{X} \geq T_{st} \Rightarrow \\ &m\ddot{X} \geq \mu_{st} N \Rightarrow \\ &m\ddot{X} \geq \mu_{st} mg\left(1+\frac{\ddot{V}}{g}\right) \Rightarrow \\ &\ddot{U} \geq \mu_{st} g\left(1+\frac{\ddot{V}}{g}\right) \end{aligned}$$

Ignoring the vertical ground motion (the vertical acceleration) then sliding takes place only in case of:

$$\ddot{U} \geq \mu_{st} g \tag{1.8}$$

1.3. Rocking Motion

As it is described above the phenomenon of the partial uplift of a structure from its foundation and its oscillation when the center of rotation changes simultaneously from one point of reference to another is known in the literature as rocking. It has been proved that rocking

initiates when during the excitation occurs $\ddot{u}_g \geq a_{g,\min} = g\tan\alpha$, where tanα=h/b and 2h, 2b are the height and width of a rectangular body. In this master's dissertation we have assume that there is no sliding. This assumption means that $\tan\alpha<\mu_{st}$ which is acceptable in the majority of structures which are significant for a Civil Engineer. If $\tan\alpha>\mu_{st}$ then the body is not rocking and consequently is sliding. Structures with $\tan\alpha>\mu_{st}$ is not examined here.

The rocking motion is usual in free-standing body and generally in free-standing structures due to the above observation. For this reason, for more than a century the response of rigid blocks allowed to uplift and rock on a rigid foundation under seismic ground motion excitation has been studied. Housner demonstrated that large rigid blocks and large rocking rigid frames is difficult to overturn dynamically. In the same way Housner has shown a scale effect that characterizes the response of rocking blocks subjected to a ground motion. For a given earthquake, larger objects need a larger ground acceleration to overturn and longer dominant period earthquakes have a larger overturning capability that shorter dominant period ones. This explains the survival of ancient Greek and Roman top-heavy temple structures in regions of high seismicity, despite the lack of historical evidence that ancient engineers were aware of the size effect of rocking structures. This size effect has lead researchers to propose rocking as a seismic response modification technique. A 60-m-tall bridge designed to rock has already been built across the Rangitikei River in New Zealand in 1981. Moreover, a 33-m-tall chimney at the Christchurch New Zealand airport has been designed to uplift. Furthermore, three 30 to 38-m-tall chimneys in Piraeus, Greece, have been retrofitted by letting them uplift in case of an earthquake.

Although the phenomenon has been studied there are questions and problems that require further research and verification with the reality. On the other hand due to the Finite Element Method problems that are more complicated can be solved. For this reason getting started from problems that are simple and understanding the motion of a rocking block can have models that approach the real response of rocking structures.

1.4. Overturning of Solitary Blocks

Sliding and rocking are two ways that a free-standing block can respond to a base movement or a ground motion. The most significant questions researchers try to solve are when a

structure is overturning and when is rocking, in what accelerations are stable, why slender structures have survived the earthquakes, in what way can take place an overturning and how can we protect ancient monuments if we know their properties. Early studies of the response of rigid bodies have shown that a block can overturn with two different ways:

a) With one or more impacts.

b) Without impact.

With reference to the following figure can understand how difficult is the approaching of the seismic response or the overturning of pillars or free-standing structures. Two pillars which was shown as same under an earthquake had different response. The one has overturned while the other is stable. The frame in the width of the picture is stable as it was expected.

Figure 2: Overturning of a free-standing pillar after an earthquake.

2. Rocking Response of Undamped Rigid Blocks

2.1. Solution of the equation of motion of an Undamped Rocking Body (URB) using standard ODE solvers available in MATLAB

It was assumed a rectangular block with height 2h and width 2b. If the coefficient of friction between the block and the base is infinite so that there is no sliding, the equation of motion of a solitary free standing block with $R=\sqrt{h^2+b^2}$ and slenderness $a=\arctan(b/h)$ under a horizontal ground acceleration $\ddot{u}_g(t)$, when rocking around the pivot points O and O′respectively is:

$$I_0\ddot{\theta}(t)+mgR\sin[\alpha\,\mathrm{sgn}\,\theta(t)-\theta(t)]=-m\ddot{u}_g(t)R\cos[\alpha\,\mathrm{sgn}\,\theta(t)-\theta(t)] \tag{2.1}$$

where $I_0=(4/3)mR^2$ is the moment of inertia with respect to the pivot point, g is the gravity acceleration, m is the mass of the block and θ is the response rotation.

Rocking initiates when during the excitation occurs $\ddot{u}_g \geq \mathrm{a}_{g,\min}=g\tan a$. Replacing I_0 to the above equation and defining the quantity $p=\sqrt{\frac{3g}{4R}}$ as the frequency parameter of the rocking block, equation takes the following form:

$$\ddot{\theta}(t)=-p^2\left[\sin\left[\alpha\,\mathrm{sgn}(\theta(t))-\theta(t)\right]+\frac{\ddot{u}_g}{g}\cos[\alpha\,\mathrm{sgn}(\theta(t))-\theta(t)]\right] \tag{2.2}$$

If it is assumed that θ and α are small or linearizing the equation of motion then it can be expressed in a simplified form as:

$$I_0\ddot{\theta}(t)+mgR(\alpha\,\mathrm{sgn}\,\theta-\theta)=-m\ddot{u}_gR \tag{2.3}$$

The solution of Equations is obtained numerically via a state-space formulation with standard ODE solvers available in MATLAB. With reference to Figure 3 and in order to decide among the solvers a comparison between 2 ODE solvers took place. The response of a rigid rocking

body with R=2m, slenderness ratio value tanα=0.1 and 0.333 under a symmetric Ricker pulse and a sine pulse excitation with a_p=3.6gtanα, ω_p=3π rad/s and ω_p=4.44π rad/s respectively is computed and plotted in Figure 3.

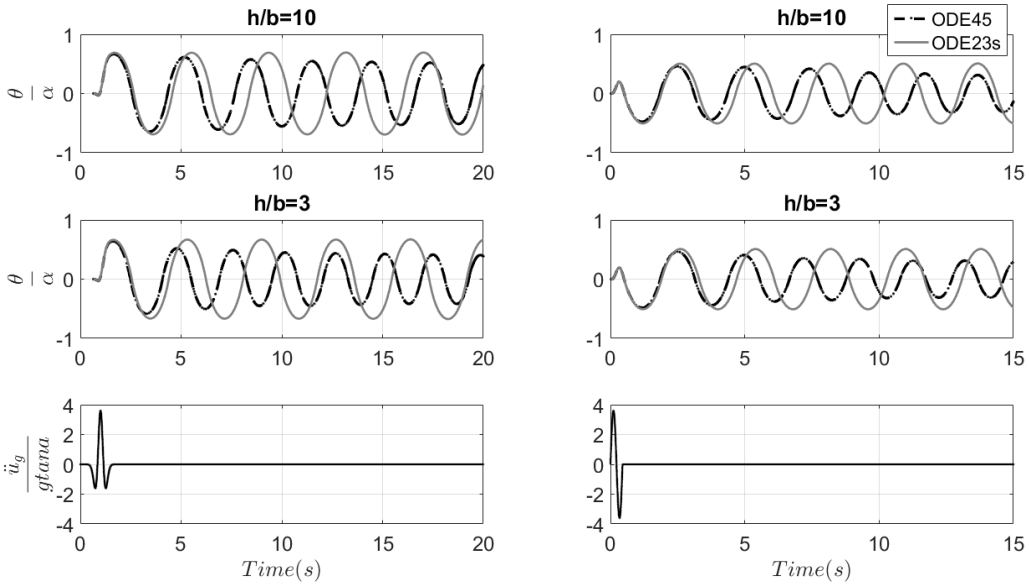

Figure 3: Comparison of rocking rotation time history response of undamped rocking bodies under a symmetric Ricker pulse (left) and to a sine pulse excitation (right) using ODE45 and ODE23s solver.

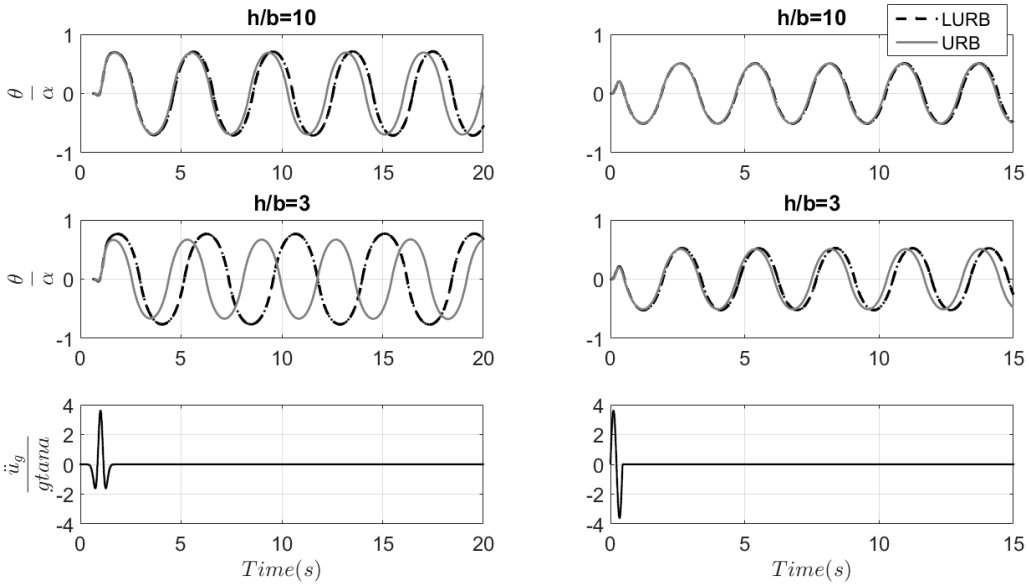

Figure 4: Comparison of rocking rotation time history response of undamped rocking bodies using full equation of motion (URB) and undamped rocking bodies with linearized equation of motion (LURB) under a symmetric Ricker pulse (left) and a sine pulse excitation (right).

The results obtained from the two ODE simulations do not match so well. Nevertheless, ODE23s solver fits the real response of rocking bodies.

In Figure 4 is presented the different response of the above blocks in case of linearization of the equation of motion. If the slenderness ratio is small ($\tan\alpha=0.1$) or θ/α is small (right) the results agree very well. For larger slenderness ratios, however, the assumption of small θ and α contains errors.

2.2. Simulations of Undamped Rocking Bodies (URB) using OpenSees and Simple Finite Element Models

If there is the assumption that a rigid body is rocking on a rigid surface, as it described previously, equations can be easily solved using a numerical computing package. The equations of more complex rocking structures or flexible rocking structures become much more complicated and their solution becomes cumbersome. Therefore, equivalent SDOF models are proposed. The models include an elastic column with cross section identical to the cross section of the rocking block connected to a zero-length non-linear elastic rotation spring. The Figure 5 *(left)* shows the moment-rotation relationship during the rocking motion of a solitary free-standing rigid block. The system has infinite stiffness until the magnitude of the applied moment reaches the value $mgR\sin\alpha$. Once the block is rocking, its restoring forces decreases monotonically, reaching zero when $\theta=\alpha$. The moment-rotation relationship was introduced in the models either taking into account the negative stiffness of the rocking block (linear spring) or considering second-order geometric transformations and large displacements (non-linear spring). In the second case, the spring has a rigid-plastic moment-rotation response envelope with yield moment equal to $mgR\sin\alpha$ and full geometric nonlinearity. For the comparison of the response between the URB and the USDOFSM the Young's Modulus, E, is set to a very large value ($E=10^{12}$kPa) because the column is quasi-rigid. In the following Figure 5 are presented the two different approaches of the moment-rotation relationship as they introduced in the models. It is noteworthy that the yield rotation for both of them and the yield stiffness for the case that the spring has a rigid-plastic moment-rotation relationship are set to very small values (10^{-5} to 10^{-12}) in order to avoid problems of convergence.

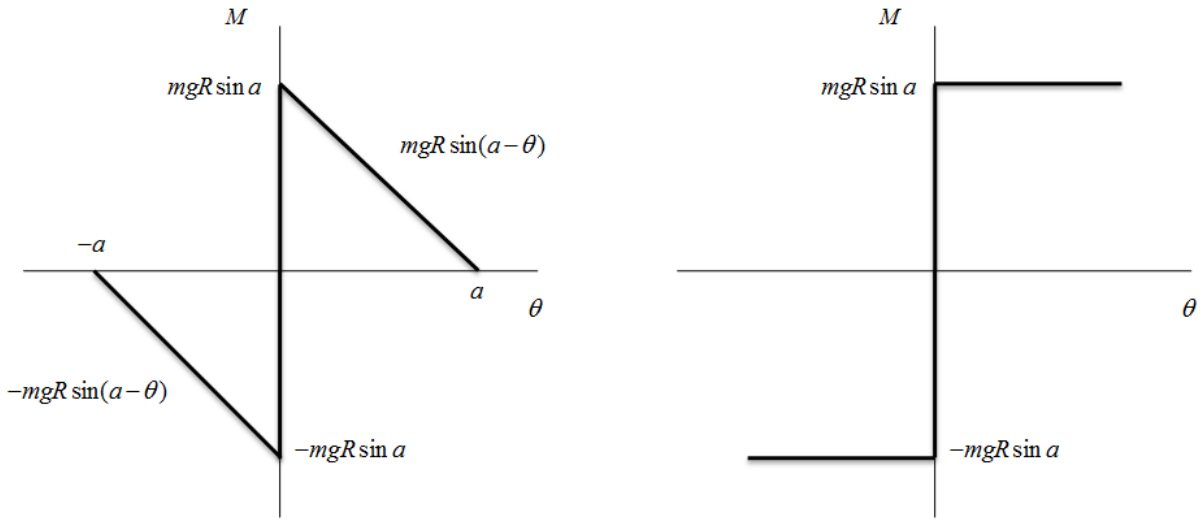

Figure 5: Moment-rotation relationships for a rigid rocking body.

2.2.1. Undamped Single Degree of Freedom Spring Model 1 (USDOFSM -1)

Initially, the Single Degree of Freedom Spring Model 1 is considering as a case study. The seismic response and specifically the rotation θ is the basic target of the model. The results obtained from the model verify the assumption as it is described below.

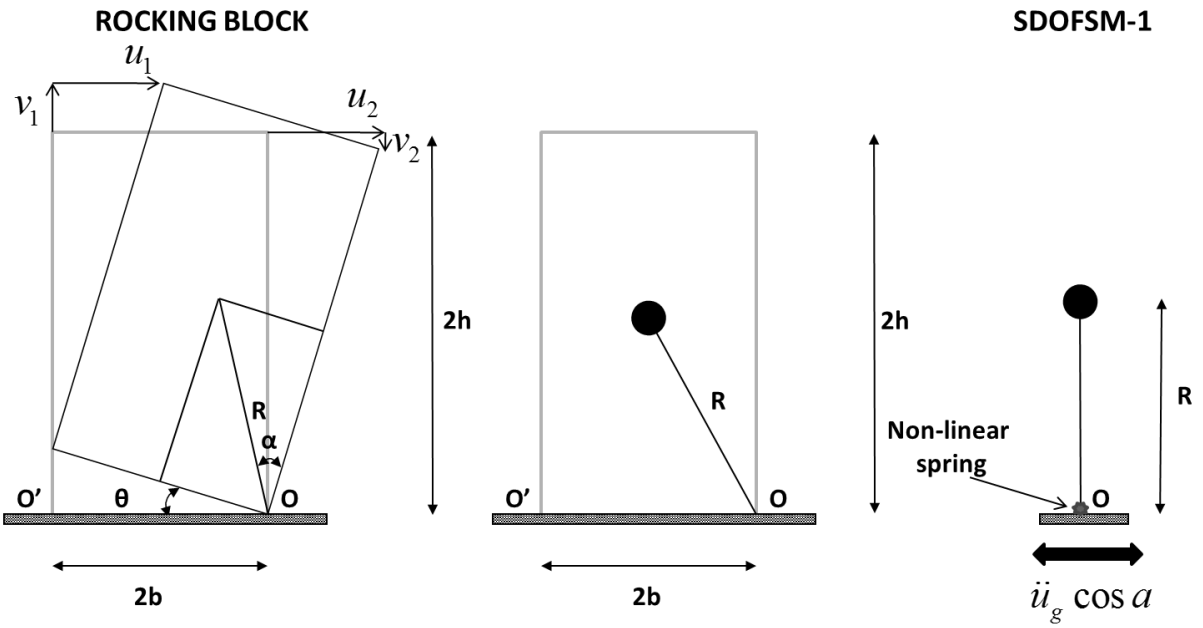

Figure 6: Rocking Block and the proposed Single Degree of Freedom Spring Model 1 (SDOFSM-1).

The equation of motion of the above spring model taking into account the negative stiffness of the rocking block is the following:

$$I_0'\ddot{\theta}(t) + mgR\sin[\alpha\,\mathrm{sgn}\,\theta(t) - \theta(t)] = -m\ddot{u}_g(t)R\cos\alpha\cos\theta \tag{2.4}$$

where $I_0' = \frac{1}{3}mR^2 + mR^2 = \frac{4}{3}mR^2 = I_0$. In comparison with the equation of motion of a Rocking Block the difference locates in the term of the horizontal ground acceleration.

The response of the Undamped Single Degree of Freedom Spring Model 1 (USDOFSM-1) in comparison with the response of a rigid rocking body with R=2m, slenderness ratio value tanα=0.1, 0.2 and 0.333 under a symmetric Ricker pulse and a sine pulse excitation with a_p=3.6gtanα, ω_p=3π rad/s and ω_p=4.44π rad/s respectively is computed and plotted in Figure 7 and Figure 8. It is noted that the small differences are most likely due to the term of the horizontal ground acceleration.

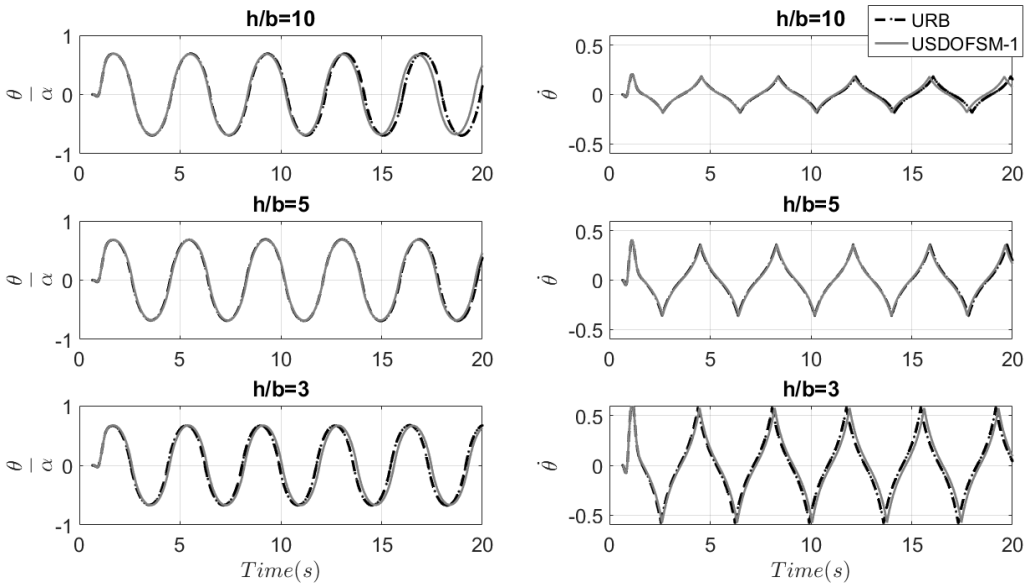

Figure 7: Comparison of rocking rotation and velocity time history response between the URB and the USDOFSM-1 to a symmetric Ricker pulse excitation.

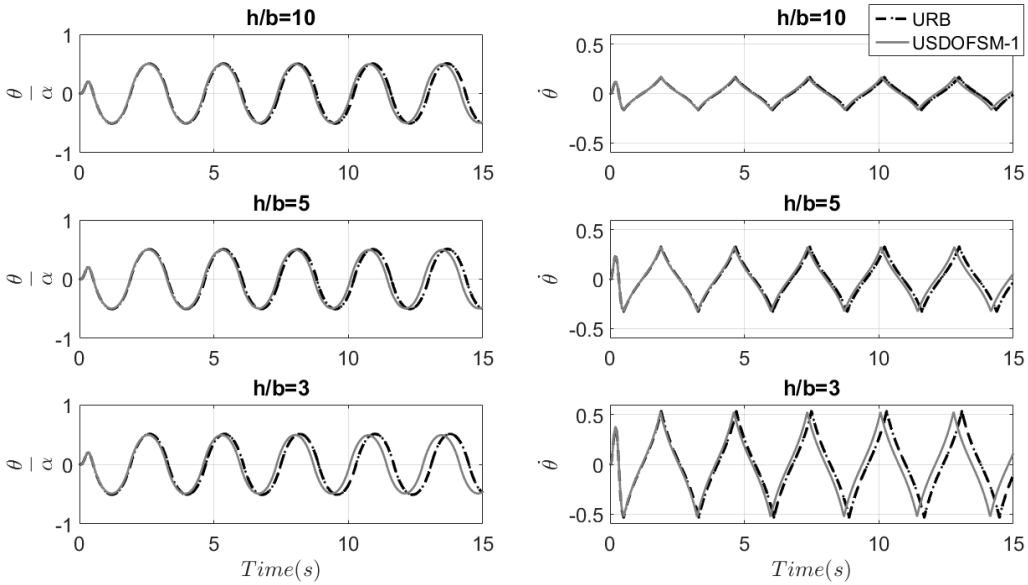

Figure 8: Comparison of rocking rotation and velocity time history response between the URB and the USDOFSM-1 to a sine pulse excitation.

2.2.2. Undamped Single Degree of Freedom Spring Model 2 (USDOFSM-2)

Secondly, an observation relevant to the equation of motion led to the Single Degree of Freedom Spring Model 2.

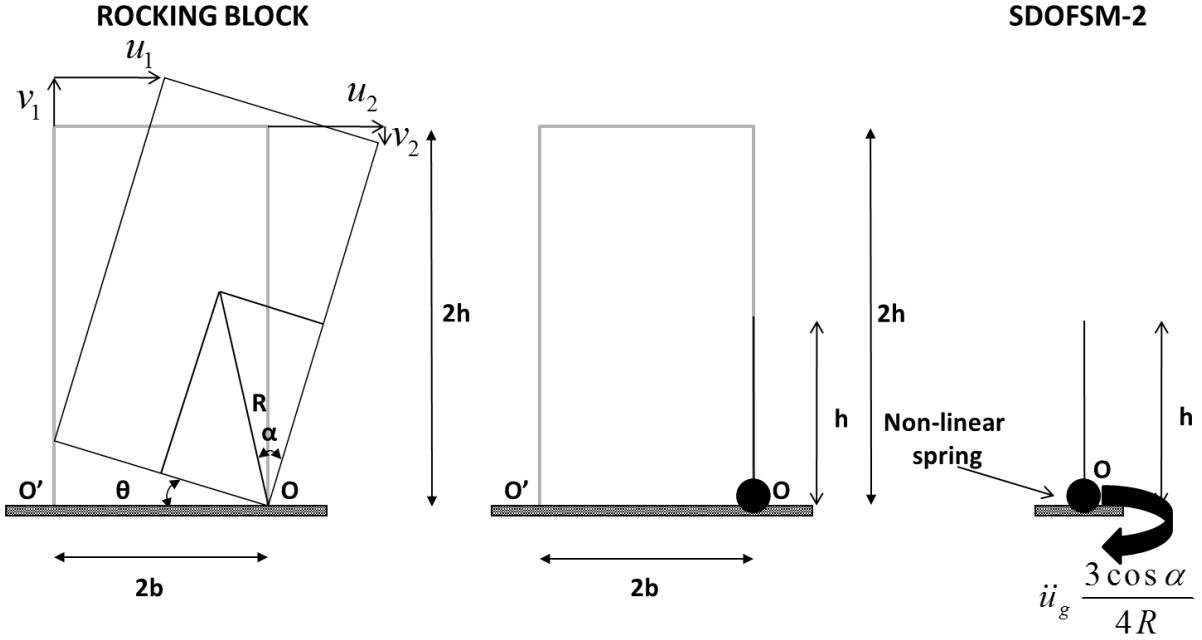

Figure 9: Rocking Body and the proposed Single Degree of Freedom Spring Model 2 (SDOFSM-2).

We can transform the equation of motion of the model in order to solve the rocking problem of a rigid block. The equation of motion of the above spring model taking into account the negative stiffness of the rocking block is the following:

$$I_0\ddot{\theta}(t) + mgR\sin[\alpha\,\mathrm{sgn}\,\theta(t) - \theta(t)] = -M_{overturning} \tag{2.5}$$

where $M_{overturning} = -I_o\ddot{u}_g\,\frac{3\cos\alpha}{4R}\cos\theta = -\frac{4}{3}mR^2\ddot{u}_g\,\frac{3\cos\alpha}{4R}\cos\theta = -m\ddot{u}_g R\cos\alpha\cos\theta$.

Considering that the term $mgR\sin[\alpha\,\mathrm{sgn}\,\theta(t) - \theta(t)]$ has introduced to the model due to the moment-rotation relationship of the rotational spring the only difference with the equation of motion of a Rocking Block is in the term of the ground acceleration. For this reason, the proposed model was modified by the direction of the ground acceleration (instead of horizontal direction the ground acceleration exerted in the rotational degree of freedom) and multiplying this term with the factor 3cosα/4R.

The response of the Undamped Single Degree of Freedom Spring Model 2 in comparison with the response of a rigid rocking body with R=5m, slenderness ratio value tanα=0.1, 0.2 and 0.333 to a symmetric Ricker pulse and a sine pulse excitation with a_p=3.6gtana, ω_p=2π rad/s and ω_p=2.66π rad/s respectively is computed and plotted in Figure 11 and Figure 12.

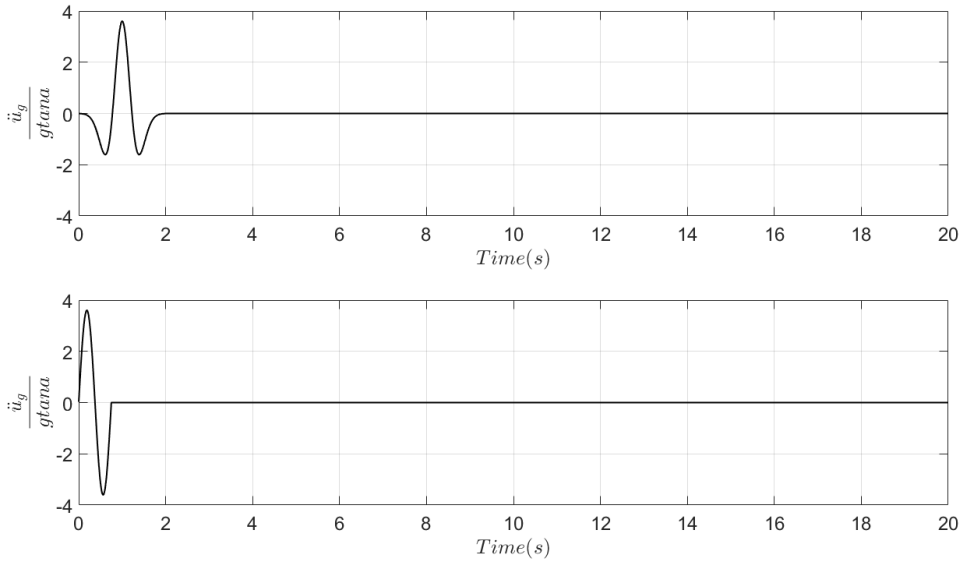

Figure 10: A symmetric Ricker pulse and a sine pulse excitation with a_p=3.6gtanα, ω_p=2π rad/s and ω_p=2.66π rad/s.

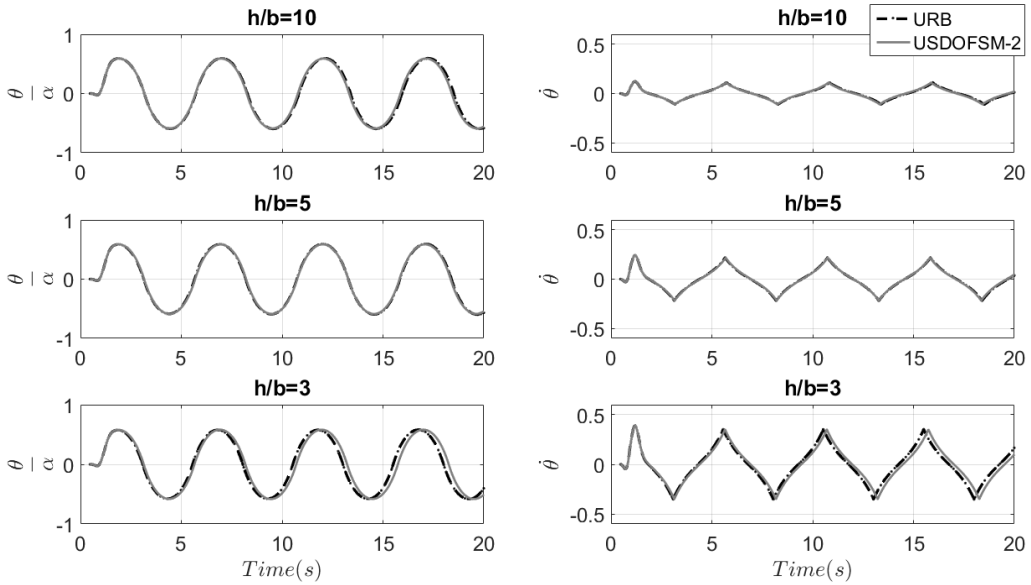

Figure 11: Comparison of rocking rotation and velocity time history response between the URB and the USDOFSM-2 to a symmetric Ricker pulse excitation.

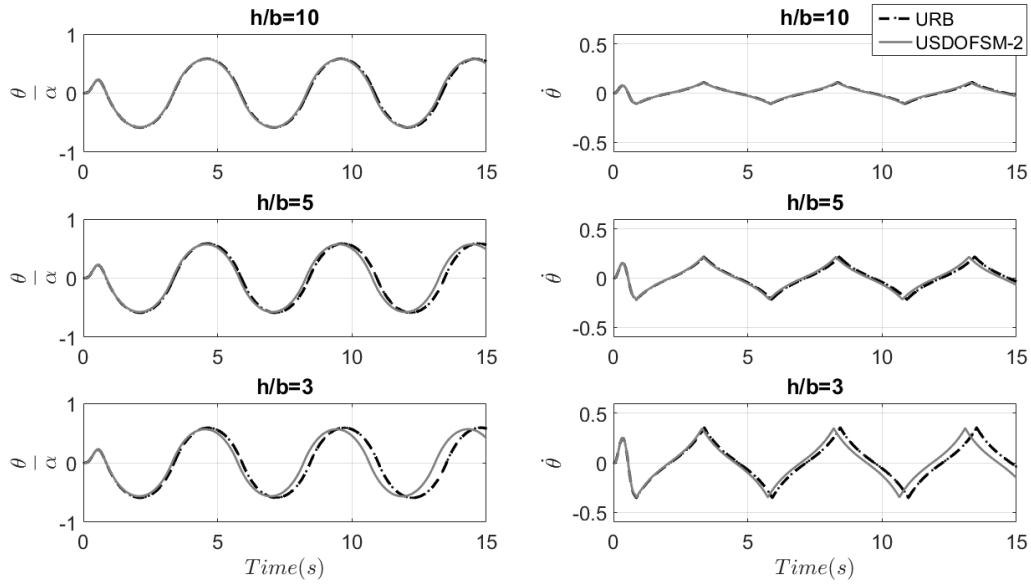

Figure 12: Comparison of rocking rotation and velocity time history response between the URB and the USDOFSM-2 to a sine pulse excitation.

2.2.3. Undamped Single Degree of Freedom Spring Model 3 (USDOFSM-3)

Subsequently, a new Single Degree of Freedom Spring Model 3 is presented. The purpose in each model is the approaching of the equation of motion of a free-standing rigid block. The

idea included the most significant term which is the moment of inertia with respect to the pivot point of the block.

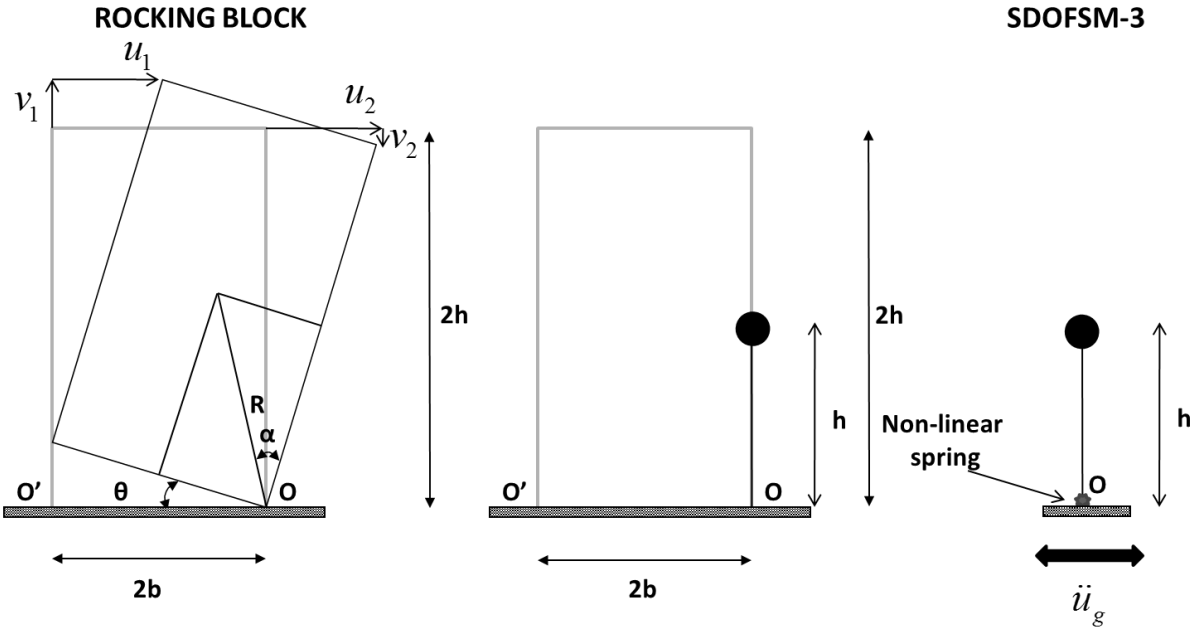

Figure 13: Rocking Body and the proposed Single Degree of Freedom Spring Model-3 (SDOFSM-3).

The equation of motion of the above spring model taking into account the negative stiffness of the rocking block is the following:

$$I_0'\ddot{\theta}(t) + mgR\sin[\alpha\,\mathrm{sgn}\,\theta(t) - \theta(t)] = -m\ddot{u}_g(t)R\cos\alpha\cos\theta \tag{2.6}$$

where $\mathrm{I}_0' = \frac{1}{3}mR^2 + mR^2\sin^2\alpha + mR^2\cos^2\alpha = \frac{1}{3}mR^2 + mR^2 = \frac{4}{3}mR^2 = I_0$

Considering that the term $mgR\sin[\alpha\,\mathrm{sgn}\,\theta(t) - \theta(t)]$ has introduced to the model due to the moment-rotation relationship of the rotational spring the only difference with the equation of motion of a Rocking Block is in the term of the ground acceleration. Consequently, the SDOFSM-3 is another way to solve the rocking problem with the Finite Element Method.

The response of the Undamped Single Degree of Freedom Spring Model-3 in comparison with the response of a rigid rocking body with R=10m, slenderness ratio value tanα=0.1, 0.2 and 0.333 under a symmetric Ricker pulse and a sine pulse excitation with a_p=3.6gtanα,

ωp=1.4π rad/s and ωp=1.905π rad/s respectively is computed and plotted in Figure 15 and Figure 16.

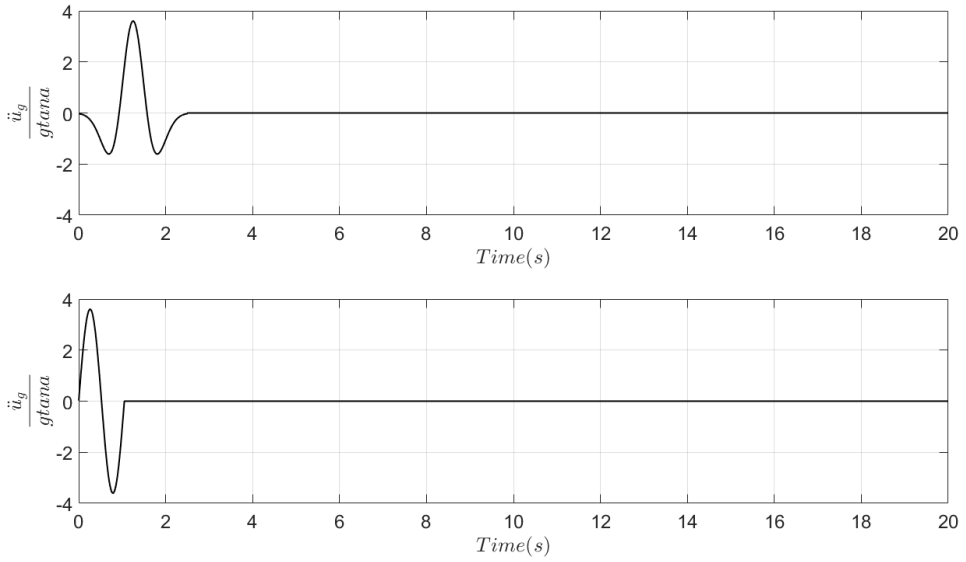

Figure 14:A symmetric Ricker pulse and a sine pulse excitation with a_p=3.6gtana, ω_p=1.4π rad/s and ω_p=1.905π rad/s.

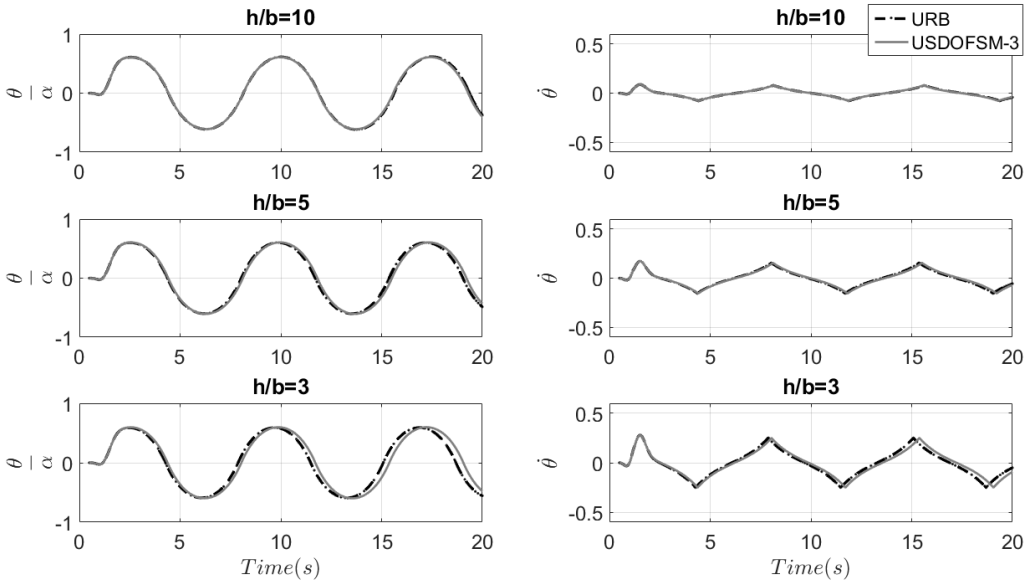

Figure 15: Comparison of rocking rotation and velocity time history response between the URB and the USDOFSM-3 to a symmetric Ricker pulse excitation.

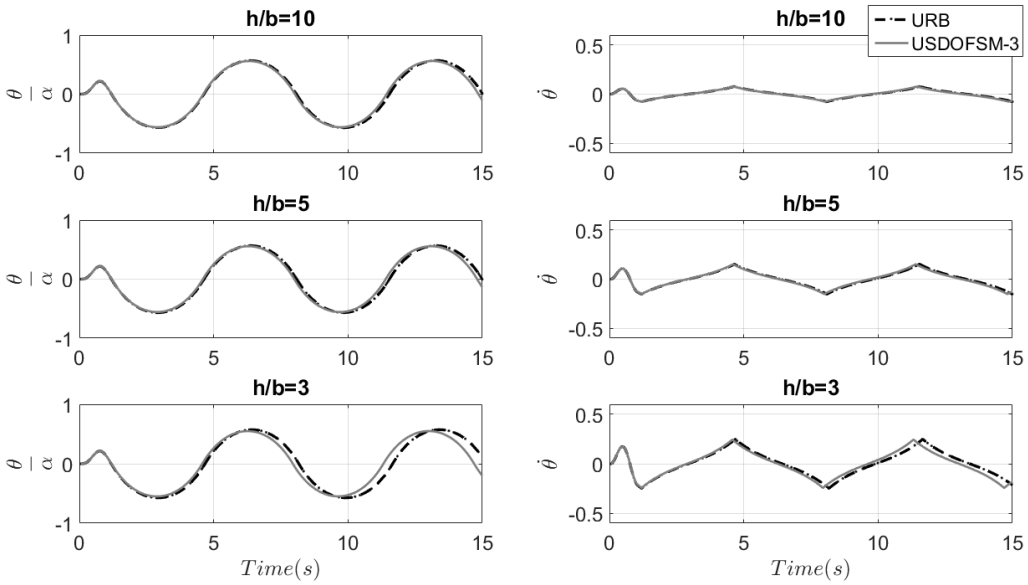

Figure 16: Comparison of rocking rotation and velocity time history response between the URB and the USDOFSM-3 to a sine pulse excitation.

2.2.4. Undamped 5-element Spring Model 4 (U5elemSM-4)

The last model emerged from the requirement of approaching the rocking response of flexible bodies. For this reason, firstly a n-element model was considered.

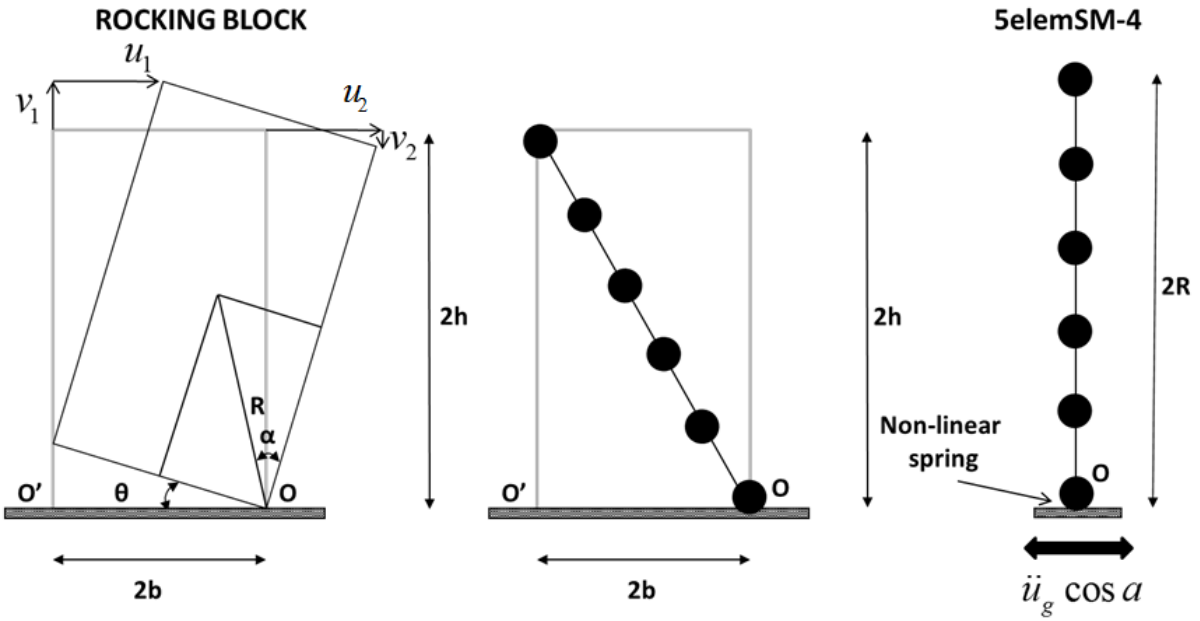

Figure 17: Rocking Body and the proposed 5-element Spring Model-4 (5elemSM-4).

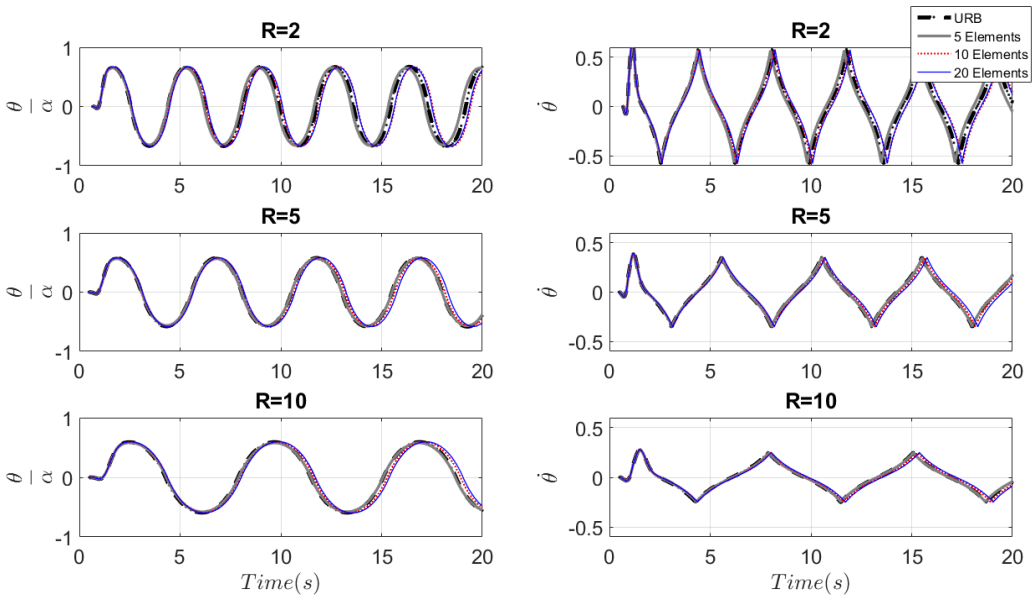

Figure 18: Confirmation of the assumption that 6 and more masses can reach the desired outcome.

After a series of analyses it was observed that a model with 6 and more masses can reach the desired outcome.

Figure 18 is presented the results obtained for 5, 10 or 20-element model for different R under a symmetric Ricker Pulse with tanα=0.3 and for $\omega_p=3\pi$ rad/s (R=2m), $\omega_p=2\pi$ rad/s (R=5m) and $\omega_p=1.4\pi$ rad/s (R=10m).

It is generally accepted that the moment of inertia of a bar rotated from his corner is $I=\frac{1}{3}mL^2$ where m is the total mass and L is the length of the bar. Taking into account the above observation, the moment of inertia of a bar with total mass m and length 2R rotated from one corner O is: $I_0^{'}=\frac{1}{3}m(2R)^2=\frac{4}{3}mR^2=I_0$. Consequently, the equation of motion of the above spring model taking into account the negative stiffness of the rocking block is the following:

$$I_0'\ddot{\theta}(t)+mgR\sin[\alpha\,\mathrm{sgn}\,\theta(t)-\theta(t)]=-m\ddot{u}_g(t)R\cos\alpha\cos\theta \qquad (2.7)$$

Once more, the only difference with the equation of motion of a Rocking Block is in the term of the ground acceleration.

The response of the Undamped 5-element Spring Model 4 in comparison with the response of a rigid rocking body with R=10m, slenderness ratio value tanα=0.1, 0.2 and 0.333 under a symmetric Ricker pulse and a sine pulse excitation with a_p=3.6gtanα, ω_p=1.4π rad/s and ω_p=1.905π rad/s respectively is computed and plotted in Figure 19 and Figure 20.

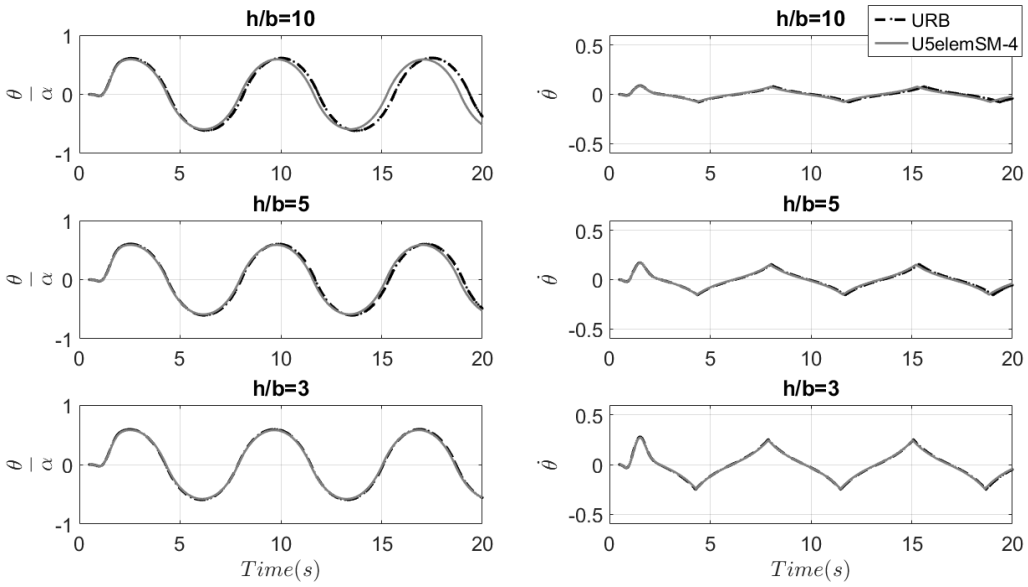

Figure 19: Comparison of rocking rotation and velocity time history response between the URB and the U5elemSM-4 to a symmetric Ricker pulse excitation.

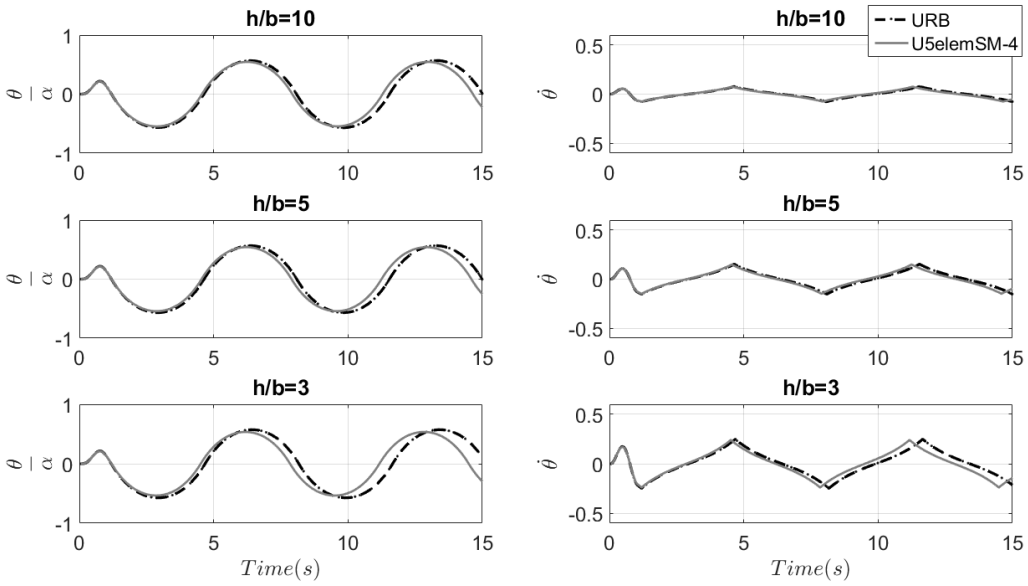

Figure 20: Comparison of rocking rotation and velocity time history response between the URB and the U5elemSM-4 to a sine pulse excitation.

2.3. Comparison of the two moment-rotation relationships

The equation of motion of the proposed Spring Models, as it was described above, considering the negative stiffness of the rocking block (disregarding damping) is:

$$I_0'\ddot{\theta}(t) + mgR\sin[\alpha\,\mathrm{sgn}\,\theta(t) - \theta(t)] = -m\ddot{u}_g(t)R\cos\alpha\cos\theta \tag{2.8}$$

The equation of motion of the proposed Spring Models 1 and 4 considering second-order geometric transformations and large displacements is:

$$I_0'\ddot{\theta}(t) + mgR(\sin\alpha\,\mathrm{sgn}\,\theta - \sin\theta) = -m\ddot{u}_g(t)R\cos\alpha\cos\theta \tag{2.9}$$

and the equation of motion of the proposed Spring Models 2 and 3 considering second-order geometric transformations and large displacements is:

$$I_0'\ddot{\theta}(t) + mgR(\sin\alpha\,\mathrm{sgn}\,\theta - \cos\alpha\sin\theta) = -m\ddot{u}_g(t)R\cos\alpha\cos\theta \tag{2.10}$$

where $I_0^{'} = \frac{4}{3}mR^2 = I_0$ for all the tree cases.

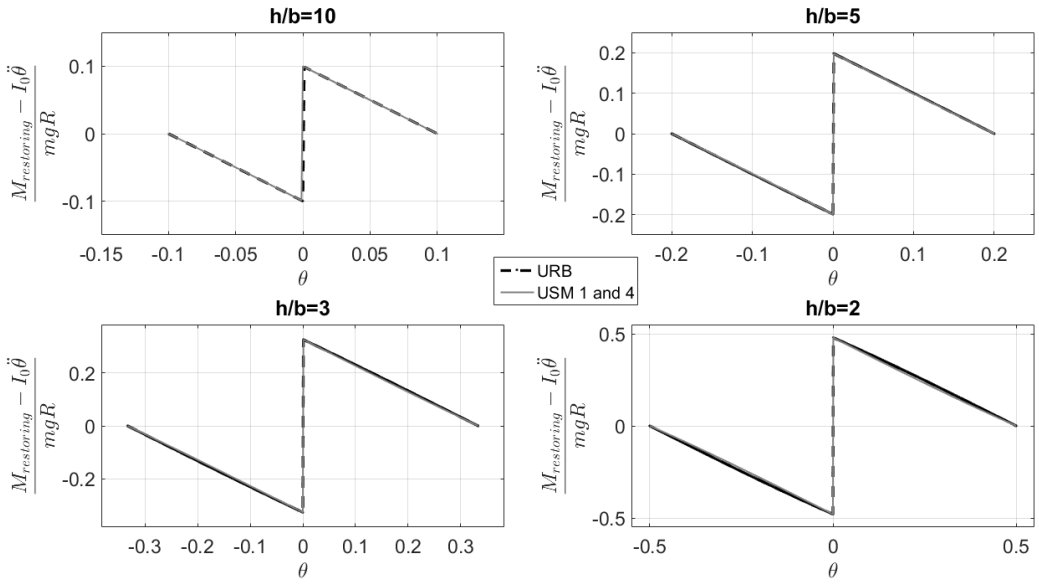

Figure 21: Comparison of the moment-rotation relationship between the RB and the SM 1 and 4 with full geometric non-linearity.

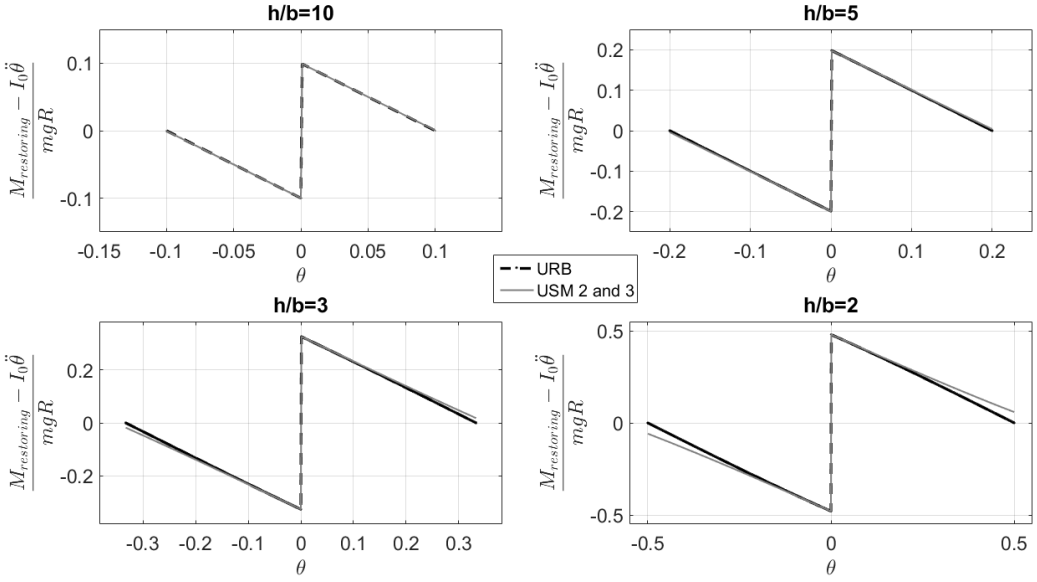

Figure 22: Comparison of the moment-rotation relationship between the RB and the SM 2 and 3 with full geometric non-linearity.

The difference between the three approaches is plotted in the Figure 21 and Figure 22.

2.4. Comparison of the displacements between the models

The horizontal and vertical displacements of the corners of the top cross section of the Rocking Body are described by the following equations:

when θ<0:

$$\begin{aligned} u_1 &= 2R\cos\alpha\sin\theta \\ u_2 &= 2R(\sin\alpha - \sin(\alpha+\theta)) \\ v_1 &= -2R\cos\alpha(1-\cos\theta) \\ v_2 &= 2R(\cos(\alpha+\theta) - \cos\alpha) \end{aligned} \tag{2.11}$$

when θ>0:

$$\begin{aligned} u_1 &= 2R(\sin\alpha - \sin(\alpha+\theta)) \\ u_2 &= 2R\cos\alpha\sin\theta \\ v_1 &= 2R(\cos(\alpha+\theta) - \cos\alpha) \\ v_2 &= -2R\cos\alpha(1-\cos\theta) \end{aligned} \tag{2.12}$$

The horizontal and vertical displacements of the top cross section (height=2h) of the equivalent Single Degree of Freedom Spring Models taking into account the negative stiffness of the rocking block are described by the equivalent equations:

SDOFSM-1:
$$\begin{aligned} u_e &= 2R\sin\theta - (2R - 2R\cos\alpha)\sin\theta = 2R\cos\alpha\sin\theta \\ v_e &= 0 \end{aligned} \tag{2.13}$$

SDOFSM-2:
$$\begin{aligned} u_e &= 2R\cos\alpha\sin\theta \\ v_e &= 0 \end{aligned} \tag{2.14}$$

SDOFSM-3:
$$\begin{aligned} u_e &= 2R\cos\alpha\sin\theta \\ v_e &= 0 \end{aligned} \tag{2.15}$$

5elemSM-4:
$$\begin{aligned} u_e &= 2R\sin\theta - (2R - 2R\cos\alpha)\sin\theta = 2R\cos\alpha\sin\theta \\ v_e &= 0 \end{aligned} \tag{2.16}$$

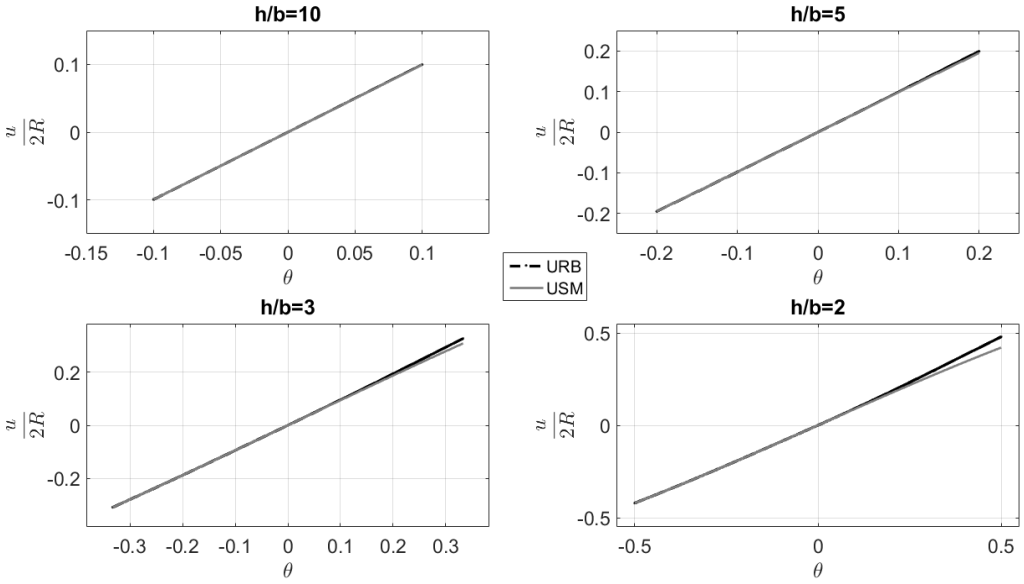

Figure 23: Comparison of the horizontal displacements of the Rocking Block and the equivalent Spring Models.

In Figure 23 was compared the equivalent horizontal displacement with the displacement of the Rocking Block and was observed that the results match well if the slenderness is up to 0.3.

In continuation of previous results, the horizontal and vertical displacements of the top cross section (height=2h) of the equivalent Single Degree of Freedom Spring Models considering second-order geometric transformations and large displacements are described by the equivalent equations:

SDOFSM-1:
$$u_e = 2R\sin\theta - (2R - 2R\cos\alpha)\sin\theta = 2R\cos\alpha\sin\theta$$
$$v_e = -2R\cos\alpha(1-\cos\theta) \quad (2.17)$$

SDOFSM-2:
$$u_e = 2R\cos\alpha\sin\theta$$
$$v_e = -2R\cos\alpha(1-\cos\theta) \quad (2.18)$$

SDOFSM-3:
$$u_e = 2R\cos\alpha\sin\theta$$
$$v_e = -2R\cos\alpha(1-\cos\theta) \quad (2.19)$$

5elemSM-4:
$$u_e = 2R\sin\theta - (2R - 2R\cos\alpha)\sin\theta = 2R\cos\alpha\sin\theta$$
$$v_e = -2R\cos\alpha(1-\cos\theta) \quad (2.20)$$

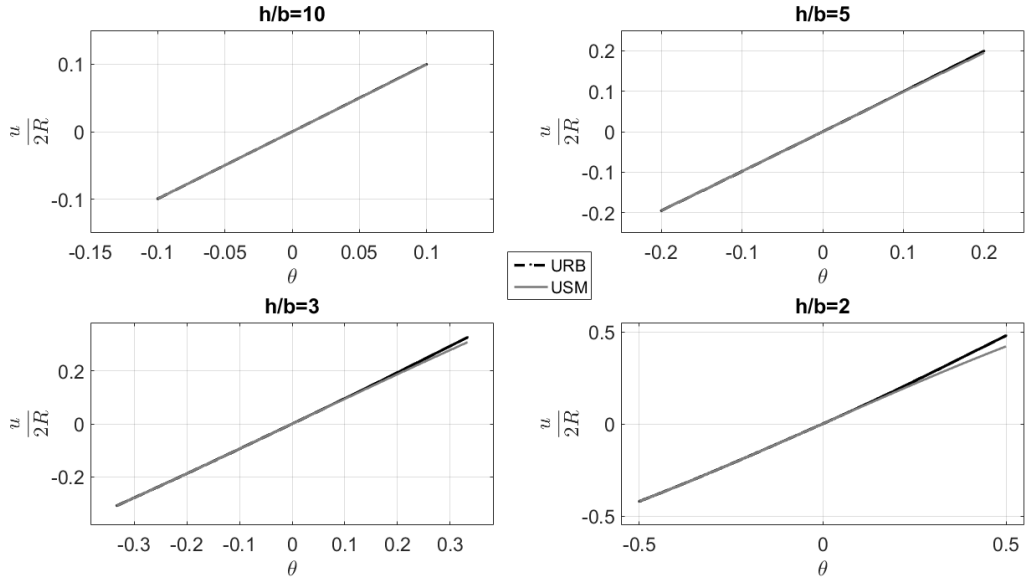

Figure 24: Comparison of the horizontal displacements of the Rocking Block and the equivalent Spring Models.

Although in the first approach the vertical displacement of the top cross section is 0, taking into account second-order geometric transformations is a way to compute the vertical

displacements (which are insignificant in comparison with the horizontal displacements). It is worth to notice that Spring Models give only negative displacements.

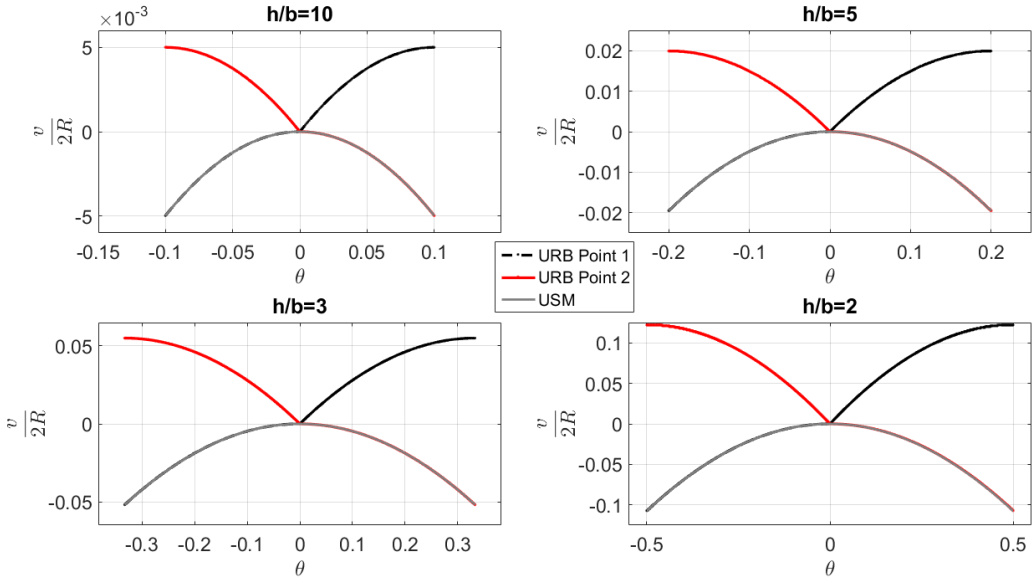

Figure 25: Comparison of the vertical displacements of the Rocking Block and the equivalent Spring Models.

2.5. Pushover Curves

The horizontal force-displacement pushover response curve for the Rocking Body (RB) with the force acting at the centroid of the block is given by:

$$\frac{F}{mg} = \tan(\alpha - \theta) \tag{2.21}$$

while the pushover curve for the equivalent Spring Models with the force acting at the node of the concentrated mass is given:

1. If the moment-rotation relationship was introduced in the models taking into account the negative stiffness of the rocking block by:

$$\frac{F}{mg} = \frac{\sin(\alpha - \theta)}{\cos\alpha \cos\theta} = \tan\alpha - \tan\theta \tag{2.22}$$

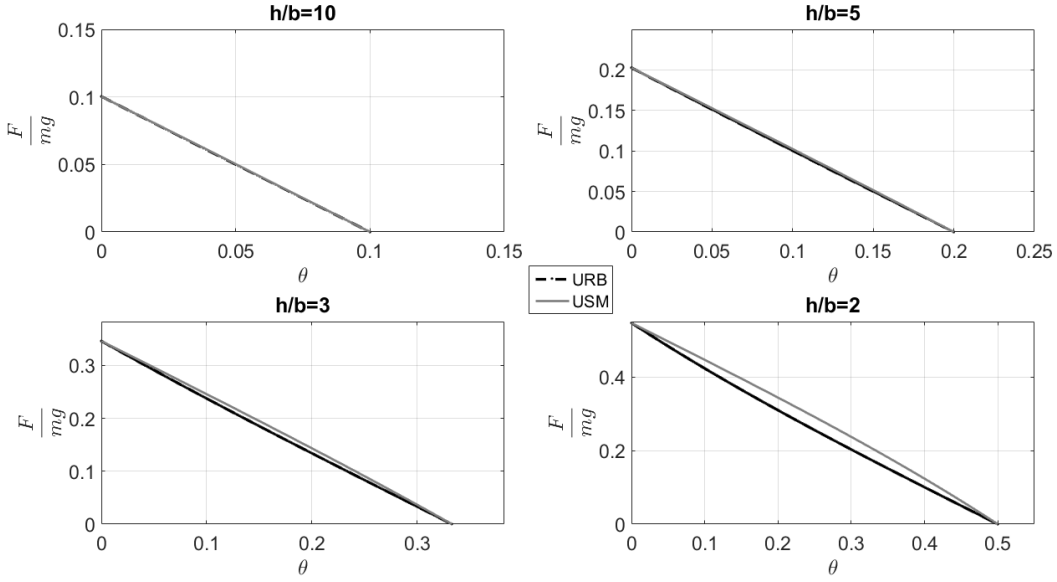

Figure 26: Force-deformation pushover curves for the RB and the SM.

2. For the models 1 and 4 if the moment-rotation relationship was introduced in the models considering second-order geometric transformations and large displacements by:

$$\frac{F}{mg} = \frac{\tan\alpha}{\cos\theta} - \frac{\tan\theta}{\cos\alpha} \tag{2.23}$$

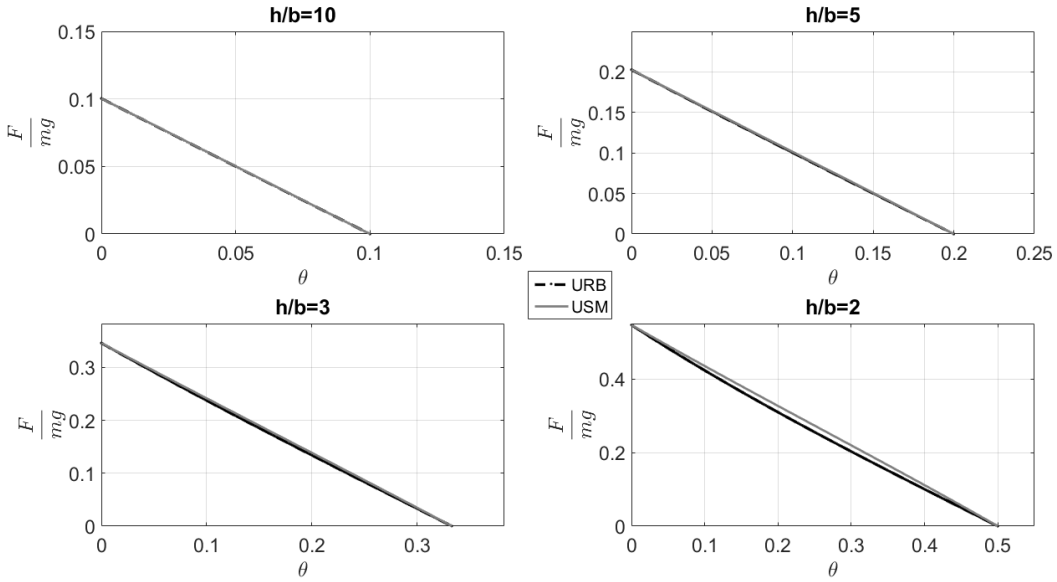

Figure 27: Force-deformation pushover curves for the RB and the SM 1 and 4.

3. For the model 3 if the moment-rotation relationship was introduced in the models considering second-order geometric transformations and large displacements by:

$$\frac{F}{mg} = \frac{\tan\alpha}{\cos\theta} - \tan\theta \tag{2.24}$$

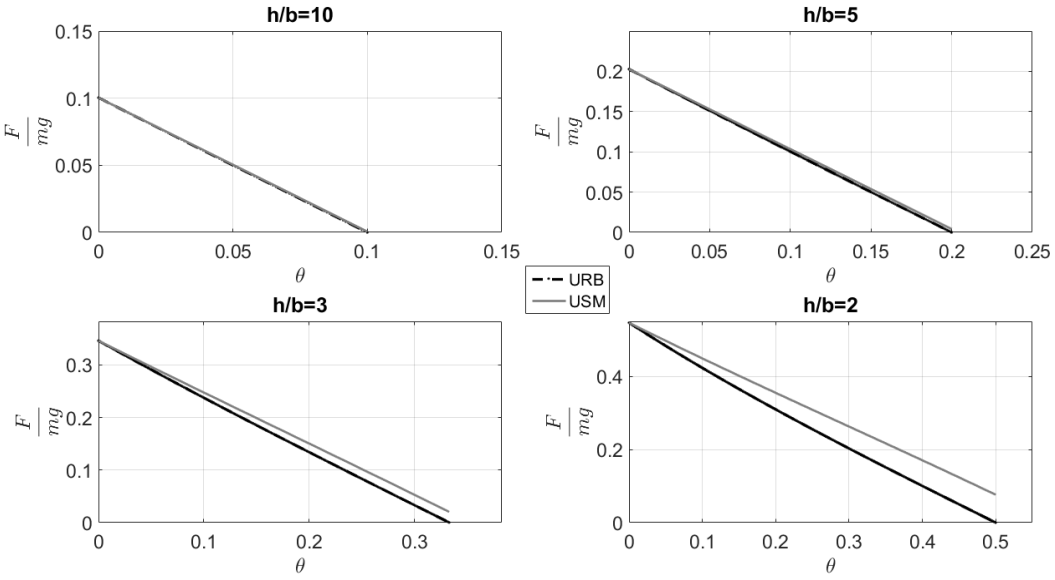

Figure 28: Force-deformation pushover curves for the RB and the SM 3.

In models 1 and 4 the assumption of full geometric non-linearity works almost perfectly in every case while in models 3 only for small slenderness up to tanα=0.2.

2.6. Comparison of the overturning moments

The equation of motion of a rocking block has arisen equalizing the restoring moment with the overturning moment. For this reason, the overturning moment is given by:

$$M_{overturning} = -m\ddot{u}_g(t)R\cos(\alpha - \theta) \tag{2.25}$$

In a corresponding manner the overturning moment of the proposed models is given by:

$$M_{overturning} = -m\ddot{u}_g(t)R\cos\alpha\cos\theta \tag{2.26}$$

The following figure represents the error which is considered as acceptable.

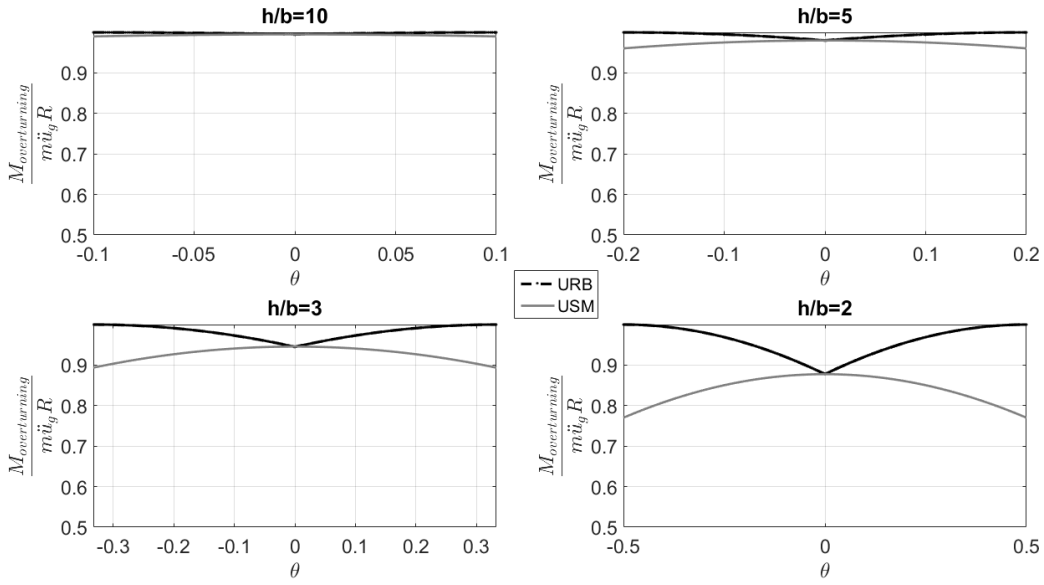

Figure 29: Comparison of the overturning moments for the RB and the SM.

3. Rocking Response of Damped Rigid Blocks

3.1. Solution of the equation of motion of a Damped Rocking Body (DRB) using standard ODE solvers available in MATLAB

Energy dissipation in rocking bodies takes place instantaneously at each impact, when the rotation changes sign at θ=0. The per-cycle of free vibration energy dissipation for a rigid rectangular block is described by the restitution factor r and is independent of the amplitude of vibration. The ratio of the energy after one complete cycle, E, to the initial energy, E_0 is:

$$\frac{E}{E_0} = r^2 = \left(1 - \frac{3}{2}\sin^2\alpha\right)^4 \tag{3.1}$$

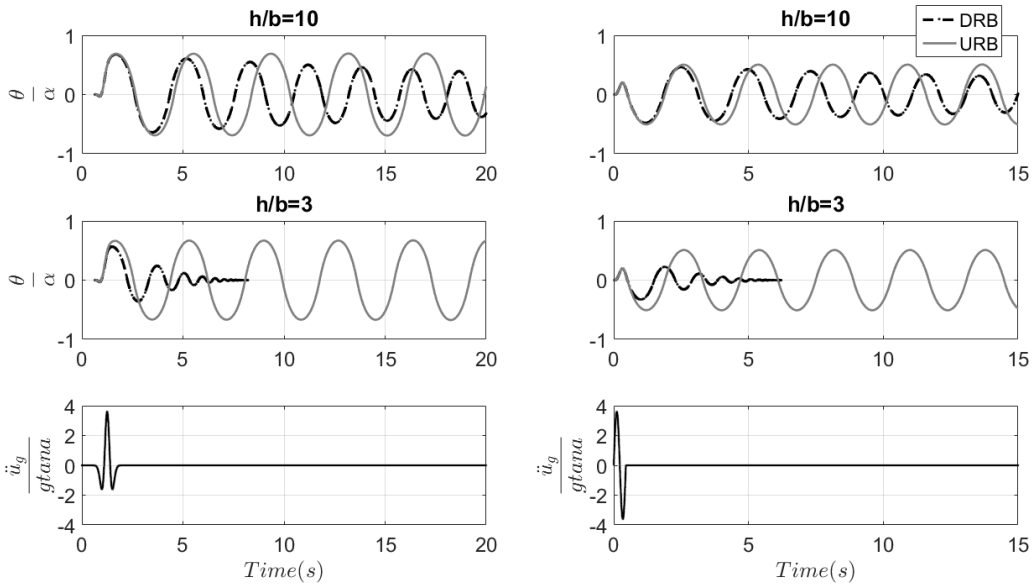

Figure 30: Influence of the coefficient of restitution to the response of a Rocking Body with R=2m under a symmetric Ricker pulse with a_p=3.6gtanα and ω_p=3π rad/s (left) and a sine pulse excitation with a_p=3.6gtanα and ω_p=4.44π rad/s (right).

In most cases, impact is described by a resulting coefficient of restitution that relates the post-impact angular velocity $\dot{\theta}^+$ to the pre-impact angular $\dot{\theta}^-$ velocity and is:

$$\eta = \frac{\dot{\theta}^+}{\dot{\theta}^-} = 1 - \frac{3}{2}\sin^2\alpha \tag{3.2}$$

3.2. Simulations of damping at Damped Spring Models with a rotational damper

As it is described above energy dissipation in rocking blocks takes place instantaneously at each impact. However, viscous damping models widely used in structural dynamics, dissipate energy continuously in proportion to an associated relative velocity. Despite this fundamental difference, the proposed models, originally, utilizes a viscous damper with a damping coefficient c associated with the column rotation velocity located at the base of the column (Vassiliou, Mackie and Stojadinović, 2014). This is intended to account only for energy dissipated during impacts of the rigid body, and does not account for any additional engineered dampers. It is further assumed that, without verification, that the energy dissipated through rocking impact does not depend strongly on the flexibility of the rocking body, and thus, on the flexibility of the column in the Spring Models.

The damping in the Spring Models is also different from the Rayleigh damping model used by Wiebe et al. [27] in that it is based on equivalent viscous damping corresponding to energy dissipation in a single cycle.

It is possible to define the per-cycle equivalent energy loss damping coefficient for the rotational damper in the models as a function of the body mass, size and slenderness:

$$c = 0.02\left(\frac{\alpha}{0.1}\right)^2 mg^{0.5}R^{1.5} \tag{3.3}$$

It is noted that that the damping coefficient was calibrated for large angles of rotation and, therefore, it is suitable for overturning analyses of the blocks and for small angle uplift. On the other hand, ElGawady et al. [28] have shown that the energy dissipated in a rocking body impact depends not only on slenderness α, but also considerably on the interface material on the rocking surfaces. Further research is needed to account for the type of interface material in the equivalent viscous damper of the SM.

The time histories of the rocking response of rigid blocks with R=5m and slenderness ratio values tanα= 0.1, 0.2 and 0.333 to a symmetric Ricker pulse excitation with a_p=3.6gtanα and ω_p=2π rad/s computed using the ODE solvers and the damped Spring Models and plotted in the following Figures.

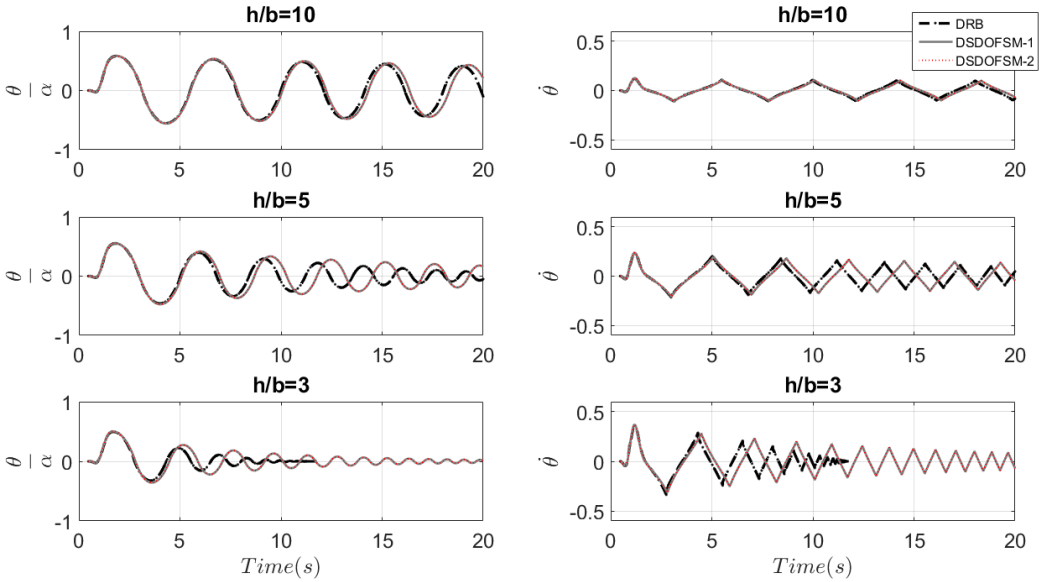

Figure 31: Comparison of rocking rotation and velocity time history response between the DRB and the DSDOFSM-1 and DSDOFSM-2 with the negative stiffness of the rocking block to a Ricker pulse excitation.

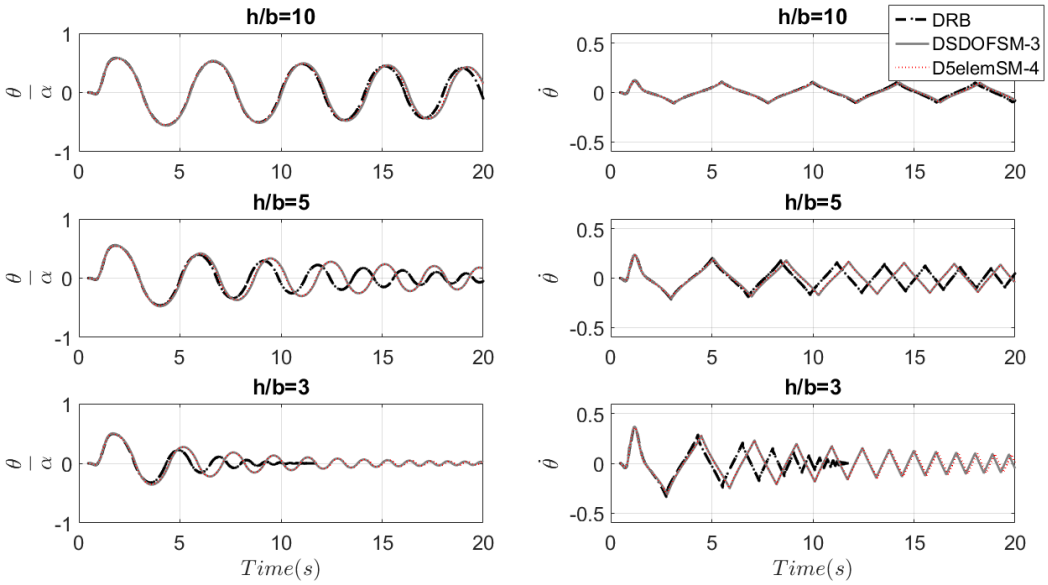

Figure 32: Comparison of rocking rotation and velocity time history response between the DRB and the DSDOFSM-3 and D5elemSM-4 with the negative stiffness of the rocking block to a Ricker pulse excitation.

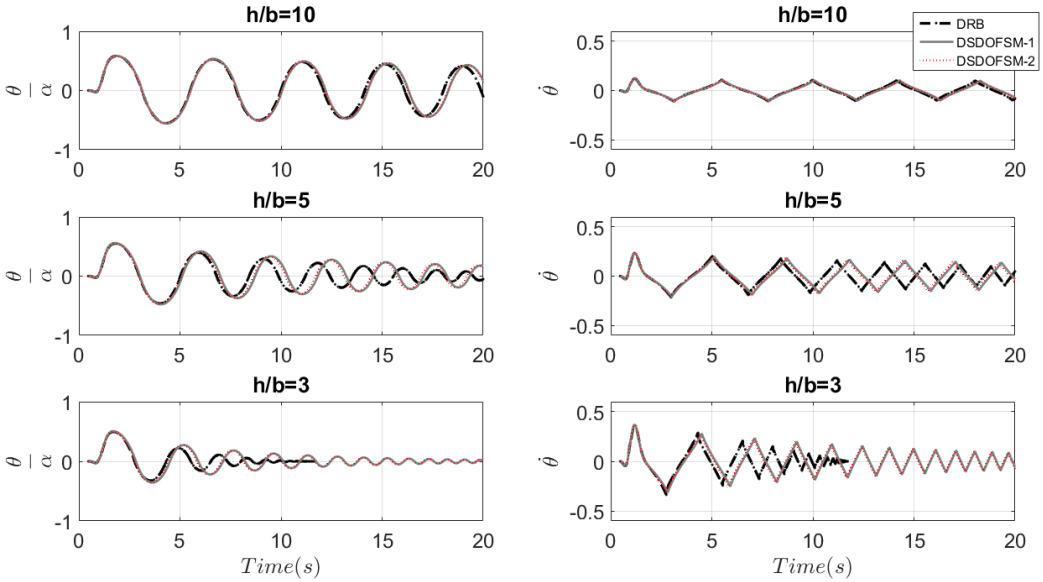

Figure 33: Comparison of rocking rotation and velocity time history response between the DRB and the DSDOFSM-1 and DSDOFSM-2 with full geometric non-linearity to a Ricker pulse excitation.

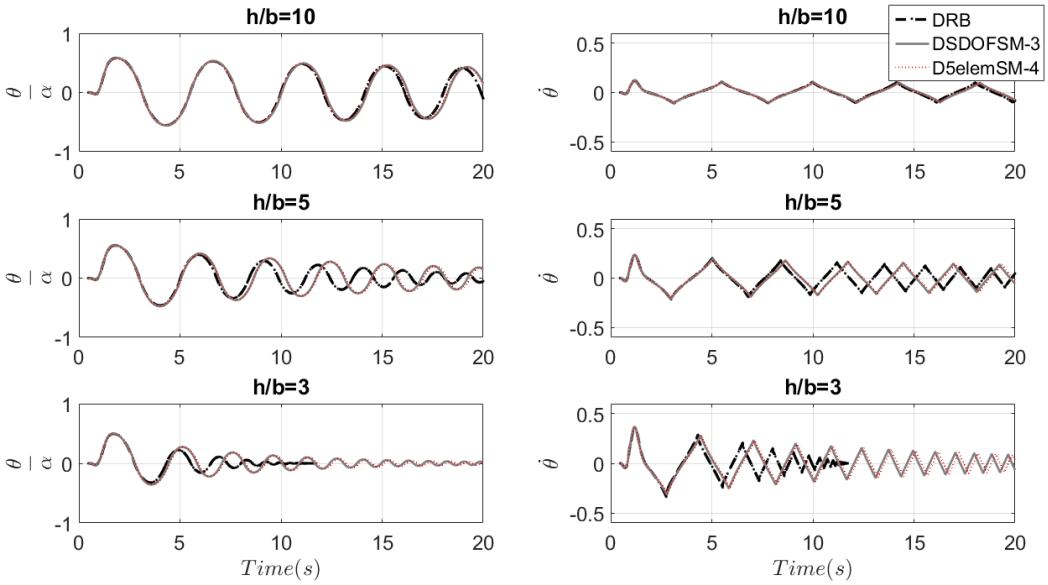

Figure 34: Comparison of rocking rotation and velocity time history response between the DRB and the DSDOFSM-3 and D5elemSM-4 with full geometric non-lineariy to a Ricker pulse excitation.

As a result, arising from the above figures, all the damped models either with negative stiffness or full geometric non-linearity give almost the same response under a pulse-like ground excitation but a response different of the Rocking Body because of the damping coefficient.

3.3. Simulations of damping at Damped 5-element Spring Model 4 using numerical damping proposed by Vassiliou, Mackie and Stojadinović (2016)

Vassiliou, Mackie and Stojadinović, 2016, proposed a model intended to facilitate a numerical time history analysis of the in-plane response of rocking structures to earthquake ground motion excitation. Assuming that no additional devices such as fuses, post-tensioned cables or dissipaters are used so that the rocking motion at the rocking interface is free the model had two components: (1) a finite element model of the solitary RB and (2) a set of requirements for conducting the time step integration and the geometric transformations during the time history solution process.

In order to model the rocking surface at the end of the rocking body a simplified version of the model proposed by Barthes [29] was used. A rocking surface was modeled using the OpenSees zero-length fiber cross-section element placed between the node j of the block and the node i of the surface. The fiber material is non-linear, with no resistance in tension and an elastic response in compression and defined using a stress/displacement relation. As a result the material constant has units of force/length^3 and is equivalent to a Winkler soil spring. No dampers are used while the fiber material is non-dissipative.

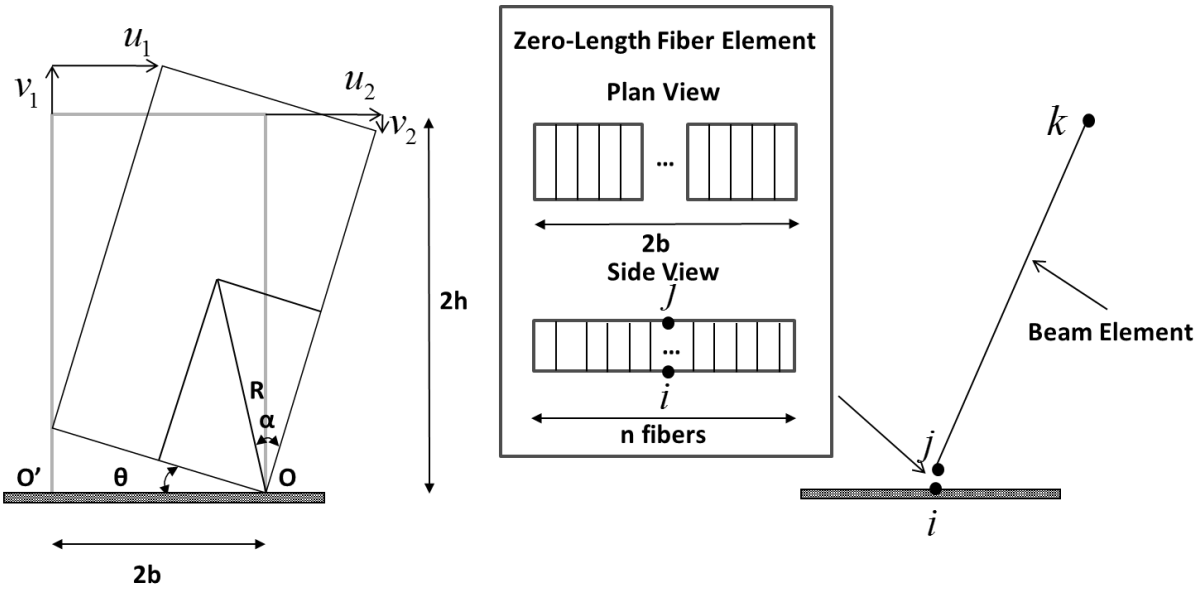

Figure 35: A solitary rigid rocking block (left) and the proposed by Vassiliou, Mackie and Stojadinović model (right).

There is the assumption that rotations and displacements are small and the OpenSees zero-length element computes the relative displacement between two nodes. The error in modeling the horizontal displacement of the bottom node of the block is evident but is insignificant when the model is used to simulate rocking response.

On the other hand the rocking body is modeled using beam-column finite elements. The current implementation of the Deformable Rocking Body model in OpenSees utilizes linear elastic beam-column elements. In order to represent rocking of a rigid body on a rigid surface the stiffness of the fibers used to model the rocking surface and the stiffness of the beam element material used to model the rocking body should be set to sufficiently large values. It is noted that the stiffness of the fibers has units of force/length^3 while the stiffness of the beam element has units of force/length^2 and selected such that impact forces deform the rocking body and not the rocking surface.

In this master's dissertation are proposed 4 ways for modeling a rigid rocking body. Adjusting the 5elemSM-4 with the above observations we had as a target to solve the rocking problem, which involves a wide range of nonlinear physical phenomena, and to determine the seismic response without classical or non-classical damping. For this reason, the model at each time step was computed using the corotational formulation to account for the effect of large displacements and rotations that may occur during the motion of a rocking body and numerical damping via the Hilber-Hunges-Taylor algorithm. Vassiliou, Mackie and Stojadinović based on the case of stiff enough fibers of the zero-length element and the observation that the impact at pivot points induces elastic axial and flexural shock waves that propagate into the rocking body used a dissipative time-stepping integration procedure to numerically damp out the shock waves in the beam-column element and neglecting the propagation of waves into the rocking surface. They have shown that the origination and propagation of these high-frequency small-amplitude shock waves requires a very small integration time step (10^{-4} is enough) and a very fine finite element mesh. However, in our work the finite element mesh was the same in every case relying on the 5elemSM-4 with fairly well results in comparison with Housner's model which assumes rocking motion of a rigid body on a rigid surface. For tall blocks (R=20m) and for big slenderness (0.333) there is an error which is acceptable taking into account the differences in the equation of motion and that there is non-compliance with their observation for a fine finite element mesh.

In the following figures were compared the rotation time history responses of different blocks under a Ricker pulse-like ground motion and a real record. It had been proven that the response is not sensitive to the number of fibers used to model the rocking surface and to the variation of the integration time step as long as it is reasonably short with respect to the period of the dominant motion components. In addition, it is noted that the numerical damping is maximum for the parameter of the OpenSees HHT algorithm a_d=2/3 and zero for a_d=1.

The most significant of this method is that the model can be used to investigate the rocking response of deformable rocking bodies, complex assemblies of rigid bodies and rocking frames comprised of deformable bodies.

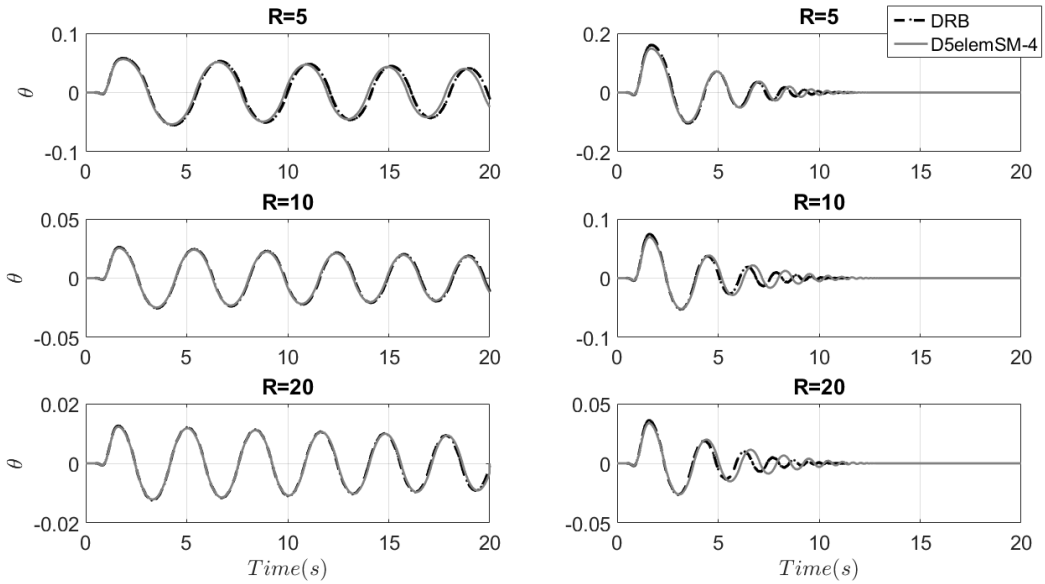

Figure 36: Comparison of rocking rotation time history response between the DRB and the D5elemSM-4 to a Ricker pulse excitation with a_p=3.6gtana and ω_p=2π rad/s using numerical damping.

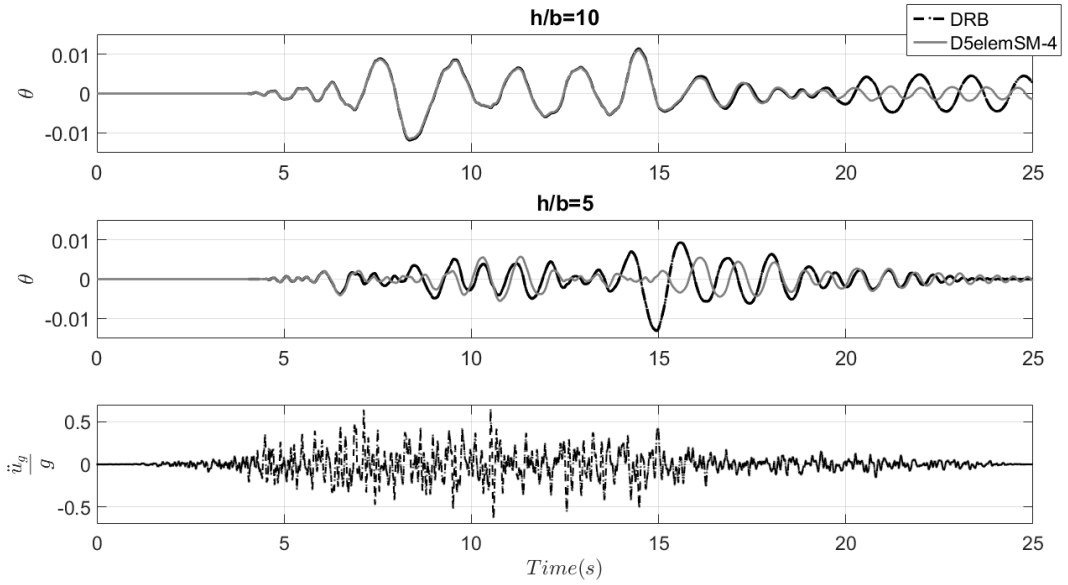

Figure 37: Comparison of rocking rotation time history response between the DRB and the D5elemSM-4 with R=10m under the Loma Prieta's 1989 earthquake (Station: Waho, φ=90º, PGA=0.638g) using numerical damping.

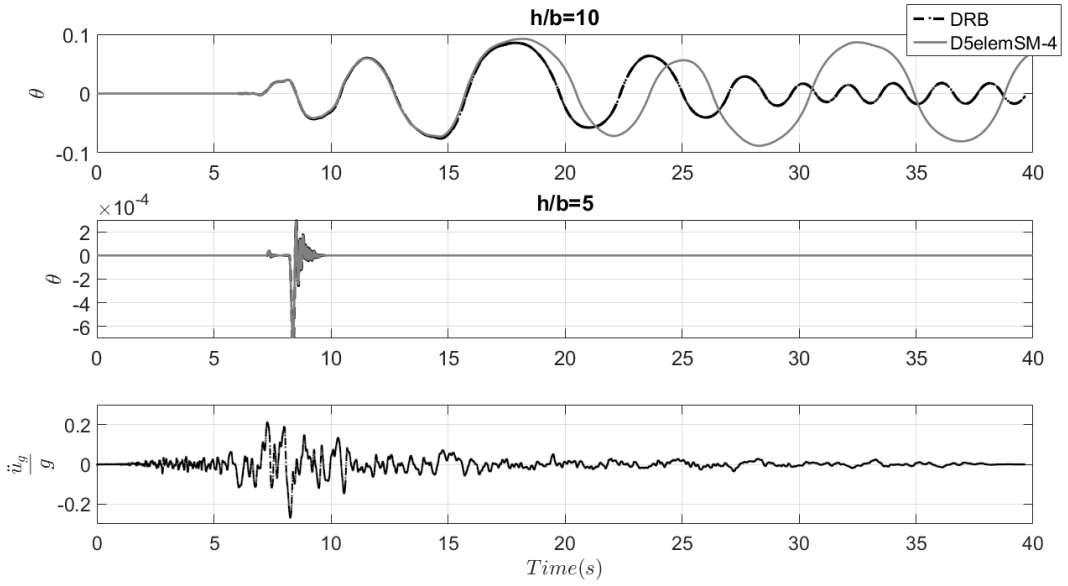

Figure 38: Comparison of rocking rotation time history response between the DRB and the D5elemSM-4 with R=5m under the Loma Prieta's 1989 earthquake (Station: Hollister Diff Array, φ=165º, PGA=0.268g) using numerical damping.

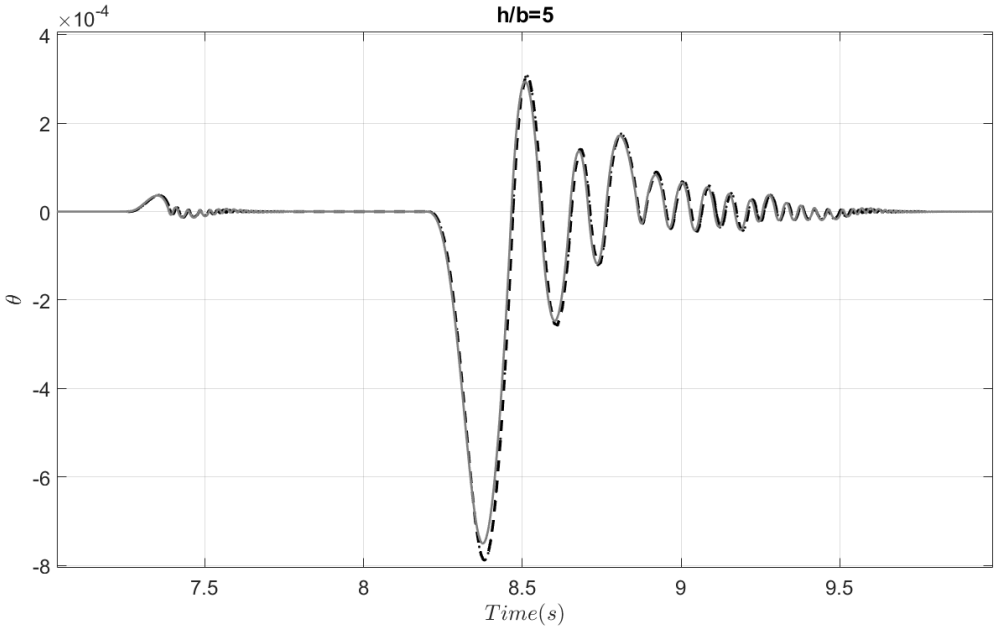

Figure 39: Zoom of the comparison of rocking rotation time history response between the DRB and the D5elemSM-4 with R=5m and h/b=5 under the Loma Prieta's 1989 earthquake (Station: Hollister Diff Array, φ=165°, PGA=0.268g) using numerical damping.

Nevertheless the seismic response in several cases is very close to the real response, there are cases with different response and the most significant disadvantage of this method is the required time of the analysis.

3.4. Simulations of damping at Damped Single Degree of Freedom Spring Models according to FEMA-356

According to FEMA-356 buildings may rock on their foundations in an acceptable manner provided the structural components can accommodate the resulting displacements and deformations. Consideration of rocking can be used to limit the force input to a building. However, rocking should not be considered simultaneously with the effects of soil flexibility. The design professional is directed to *FEMA 274* and the work of Yim and Chopra (1985), Housner (1963), Makris and Roussos (1998), and Priestly and Evison (1978) for additional information on rocking behavior. A possible procedure for considering rocking is outlined in Figure 40. The procedure involves the following steps:

• Calculation of the mass, weight, and center of gravity for the rocking system (or subsystem).

• Calculation of the soil contact area, center of contact, and rocking system dimension, *R*.

• Determination of whether rocking will initiate.

• Calculation of the effective viscous damping of the rocking system (and the corresponding design displacement spectrum).

• Calculation (graphically or iteratively) of the period and amplitude of rocking (the solution will not converge if overturning will occur—that is, when $\theta > \alpha$).

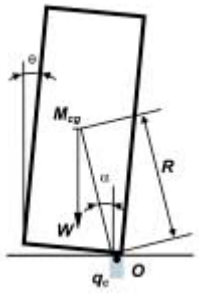

Figure 40: Rocking block as it was described by FEMA-356.

Mass, weight, and center of gravity

Note that, in general, the mass and weight will not be consistent with each other. The mass, *M*, is the total seismic mass tributary to the wall. The weight, *W*, is the vertical gravity load reaction. For the purposes of these calculations, the vertical location of the center of gravity is taken at the vertical center of the seismic mass and the horizontal location of the center of gravity is taken at the horizontal center of the applied gravity loads.

Soil contact area and center of contact

The soil contact area is taken as W/q_c. The wall rocks about point O located at the center of the contact area.

Wall rocking potential

Determine whether the wall will rock by comparing the overturning moment to the restoring moment. For this calculation, S_a is based on the fundamental, elastic (no-rocking) period of

the wall. The wall will rock if $S_a > (W/Mg)\tan\alpha$. If rocking is not indicated, discontinue these calculations.

Rocking calculations

Calculate I_o, the mass moment of inertia of the rocking system about point O.

Calculate the effective viscous damping, β, of the rocking system as follows:

$$\beta = 0.4\left(1-\sqrt{r}\right) \tag{3.4}$$

where:

$$r = \left[1-\frac{MR^2}{I_0}\left(1-\cos(2a)\right)\right]^2 \tag{3.5}$$

Construct the design response spectrum at this level of effective damping using the procedure defined in Section 1.6.1.5 of FEMA-356. By iteration or graphical methods, solve for the period and displacement that simultaneously satisfy the design response spectrum and the following rocking period equation:

$$T = \frac{4}{\sqrt{\frac{WR}{I_0}}}\cosh^{-1}\left(\frac{1}{1-\frac{\theta}{\alpha}}\right) \tag{3.6}$$

where:

$$\theta = \frac{\delta_{rocking}}{R\cos\alpha} \tag{3.7}$$

while recall that: $S_d = S_a g\frac{T^2}{4\pi^2}$

At the desired solution: $\delta_{rocking} = S_d$

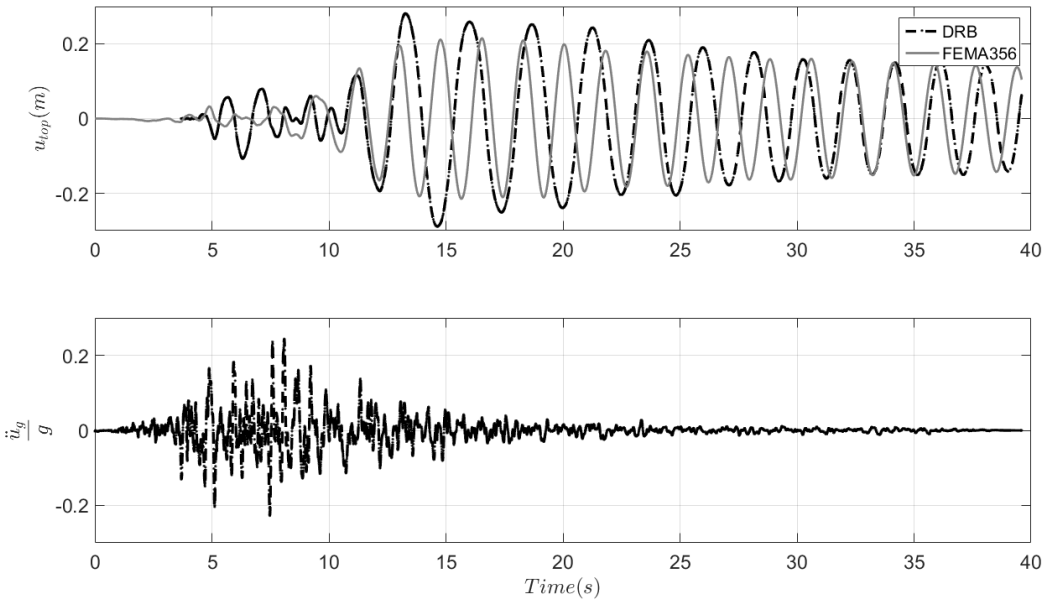

Figure 41: Comparison of rocking top displacement time history response between the DRB and the proposed by FEMA-356 model with R=5m under the Loma Prieta's 1989 earthquake (Station: Anderson Dam Downstream, φ=270º, PGA=0.235g).

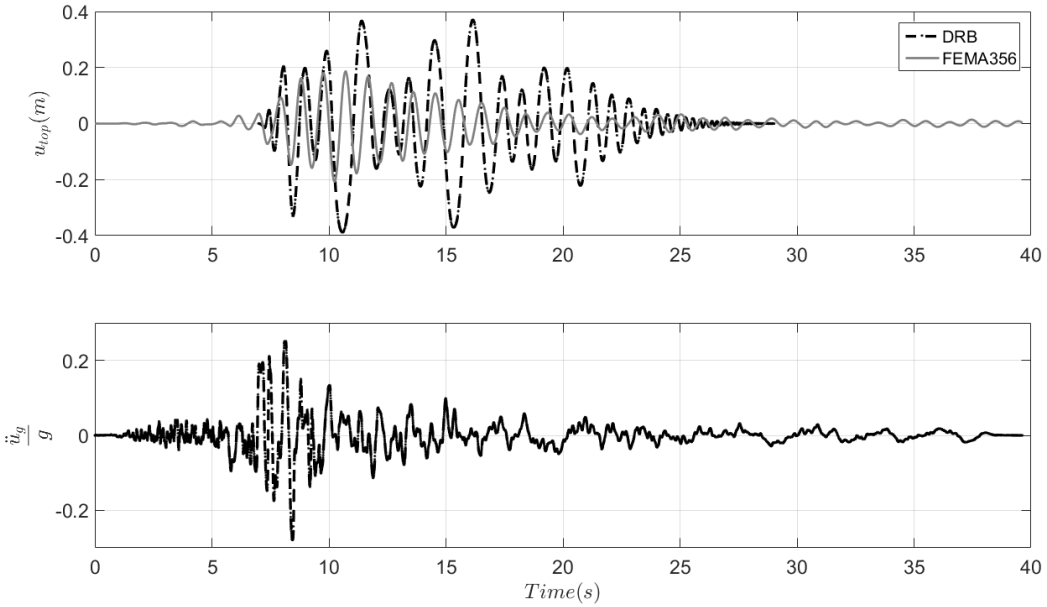

Figure 42: Comparison of rocking top displacement time history response between the DRB and the proposed by FEMA-356 model with R=2m under the Loma Prieta's 1989 earthquake (Station: Hollister Diff Array, φ=255º, PGA=0.279g).

3.5. Event-based damping proposed

A new approach of the energy dissipation in rocking blocks is proposed in this master's dissipation. The idea emerged from the fact that the energy dissipation in the rocking motion is an instantaneous event. As it is described in an above chapter the damping in the Spring Models is different from the Rayleigh damping model used by Wiebe et al [27] in that it is based on equivalent viscous damping corresponding to energy dissipation in a single cycle. Obviously, a continuous damper can approach the seismic behavior regarding the maximum rotations but it is suitable only for overturning analyses and for small angle uplift while it will always contain errors because of the hypothesis of continuous loss of energy. As a result, further research is needed to account in order to have a damping coefficient for several angles and rotations and for the type of interface material in the equivalent viscous damper of the SM.

On the other hand, if it is assumed that a rigid body is rocking on a rigid surface the coefficient of restitution that relates the post-impact angular velocity $\dot{\theta}^{+}$ to the pre-impact angular $\dot{\theta}^{-}$ velocity has been described above. Regardless of the value of the coefficient of restitution, the proposed model can approach the behavior because of the correlation of the coefficient with the angular velocity of every node. For this reason and with the assumption that energy dissipation in rocking blocks takes place instantaneously at each impact the objective was a simple work. Initially, the models proposed in chapter 2 were transformed in order to count the pre-impact velocity. Pausing the analysis in each impact and multiplying the pre-impact velocity of every node with the coefficient of restitution was calculated the post-impact angular velocity of every node. The post-impact angular velocity converted to an initial condition in order to continue the analysis (Event-Based Damping). The same procedure is repeated until the analysis stop. The following figures confirm the mass proportional damping assumption and that a finite element model can assess the seismic response of a rigid rocking block on a rigid surface.

In the following two subsections are presented several examples of blocks under pulses-like ground excitation and real records in order to convince the proposed event-based damping models works perfectly in almost every case.

3.5.1. Rocking Response under pulse-like ground excitation

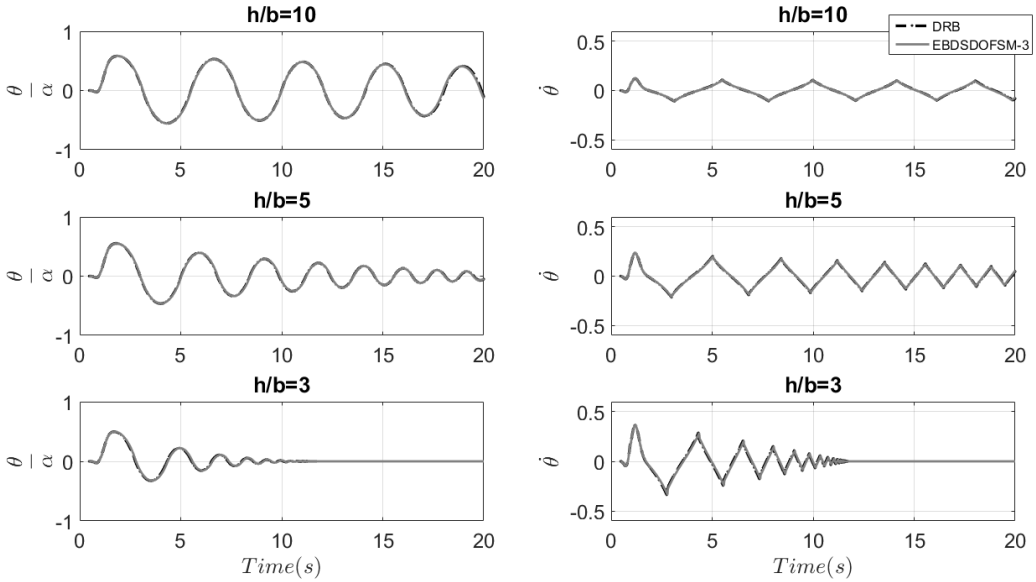

Figure 43: Comparison of rocking rotation and velocity time history response of between the DRB and the EBDSDOFSM-3 with R=5m to a Ricker pulse excitation with a_p=3.6gtana and ω_p=2π rad/s.

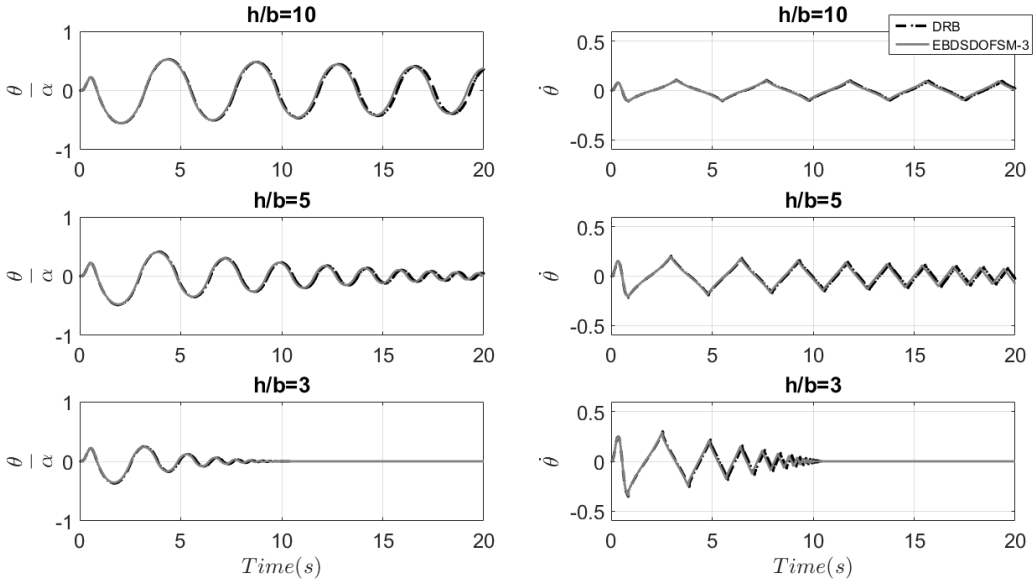

Figure 44: Comparison of rocking rotation and velocity time history response s between the DRB and the EBDSDOFSM-3 with R=5m to a sine pulse excitation with a_p=3.6gtana and ω_p=2.66π rad/s.

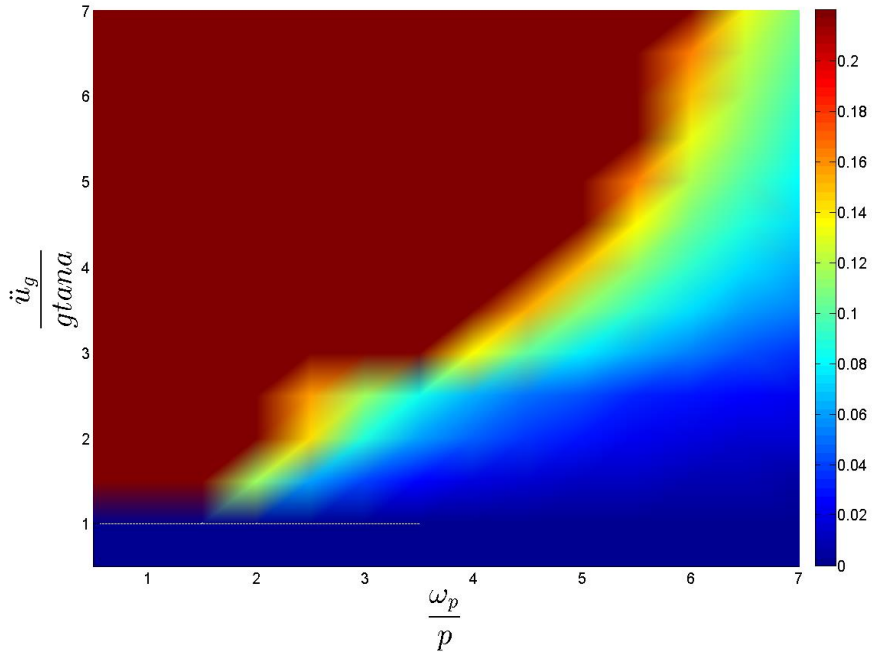

Figure 45: Overturning spectrum of damped rigid bodies under a Ricker pulse excitation.

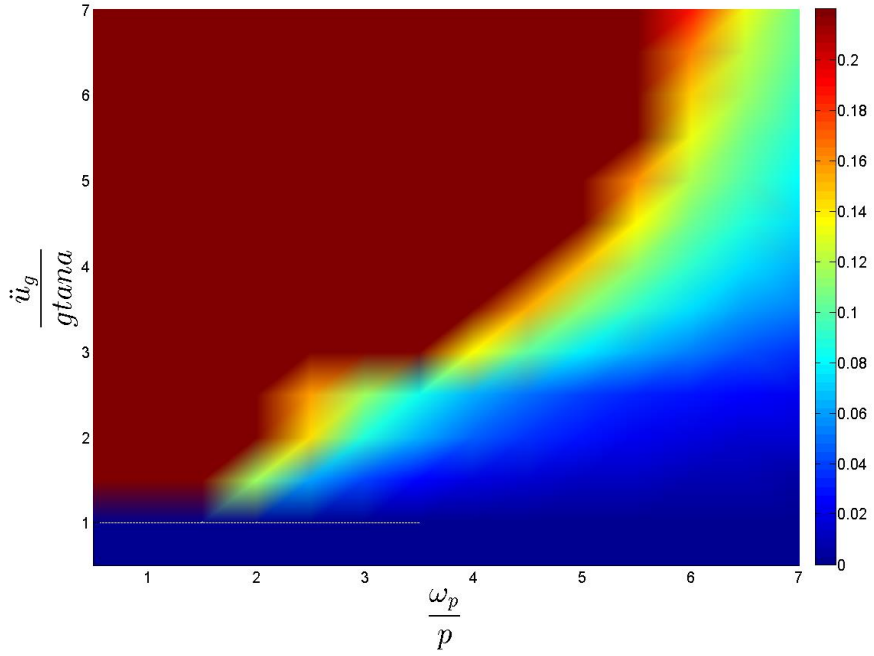

Figure 46: Equivalent overturning spectrum of the EBDSDOFSM-3 under a Ricker pulse excitation.

3.5.2. Rocking Response under real records

The event-based damping works perfectly under a pulse like-ground excitation. However, the most significant thing in a research around the seismic response of structures is the approaching under a real record. A finite element model must verify the response resulting from analytical models or experiments in order to be remarkable. In the following figures some different models under several records are tested. Although four models are proposed the results have been obtained by the SDOFSM-3 and the 5elemSM-4 aiming to confirm that either a model with one or a model with more degrees of freedom can approach the real behavior. Three models with different R or different slenderness were examined.

- Rocking Blocks with R=10m and slenderness h/b=10.

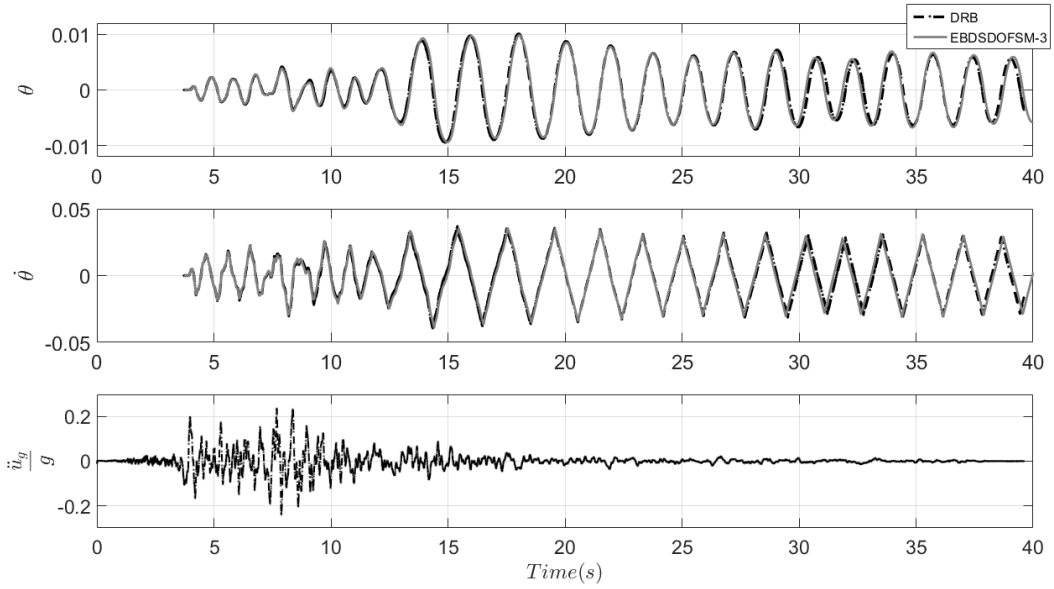

Figure 47: Comparison of rocking rotation and velocity time history response between the DRB and the EBDSDOFSM-3 with R=10m under the Loma Prieta's 1989 earthquake (Station: Anderson Dam Downstream, φ=360º, PGA=0.24g).

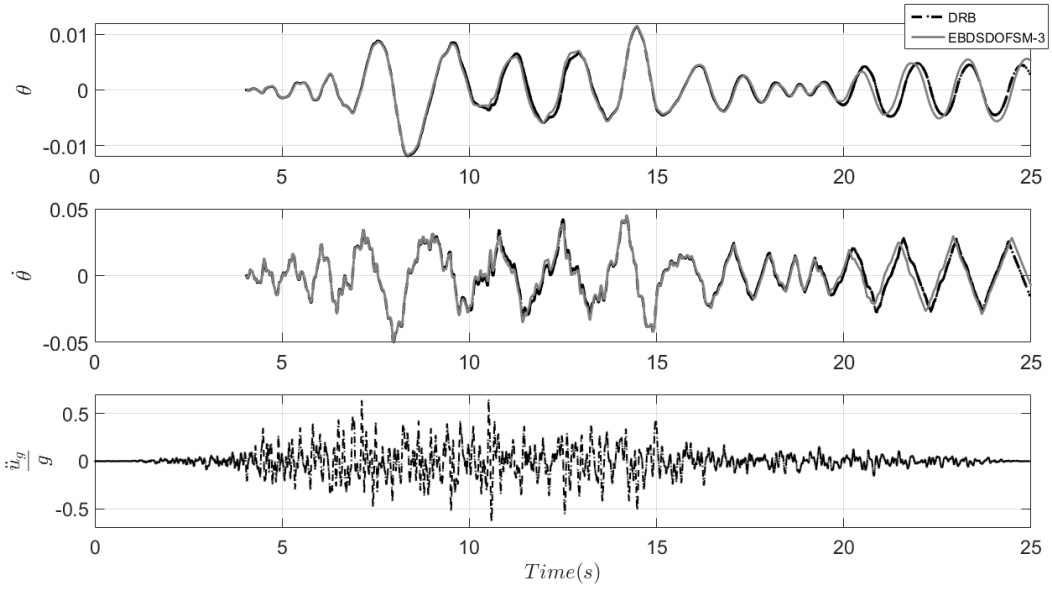

Figure 48: Comparison of rocking rotation and velocity time history response between the DRB and the EBDSDOFSM-3 with R=10m under the Loma Prieta's 1989 earthquake (Station: Waho, φ=90º, PGA=0.638g).

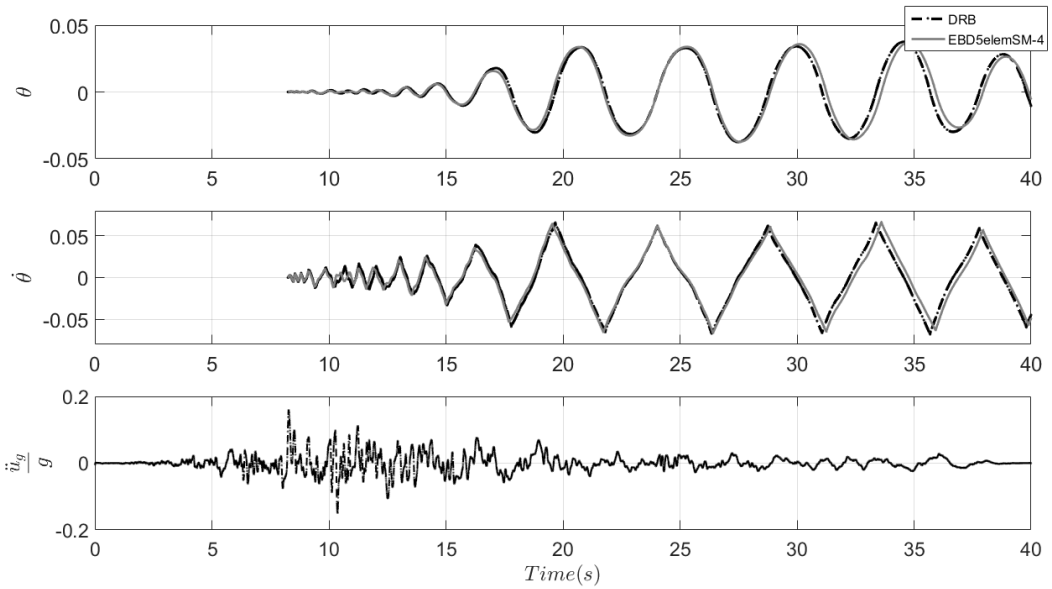

Figure 49: Comparison of rocking rotation and velocity time history response between the DRB and the EBD5elemSM-4 with R=10m under the Loma Prieta's 1989 earthquake (Station: Agnews State Hospital, φ=90º, PGA=0.159g).

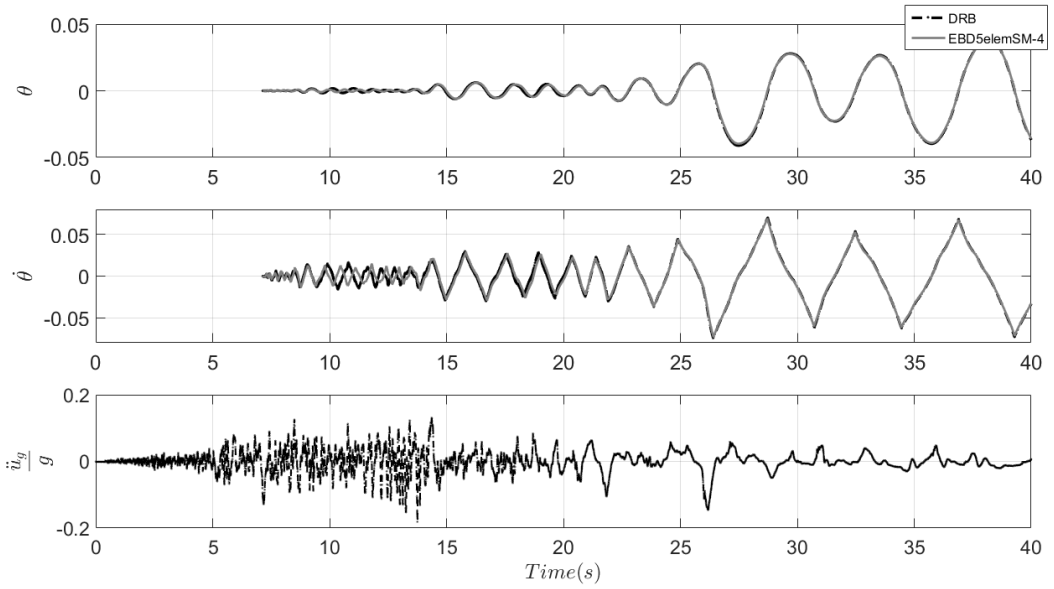

Figure 50: Comparison of rocking rotation and velocity time history response between the DRB and the EBD5elemSM-4 with R=10m under the Superstition Hills' 1987 earthquake (Station: Wildlife Liquefaction Array, φ=90^o, PGA=0.18g).

- <u>Rocking Blocks with R=5m and slenderness h/b=10.</u>

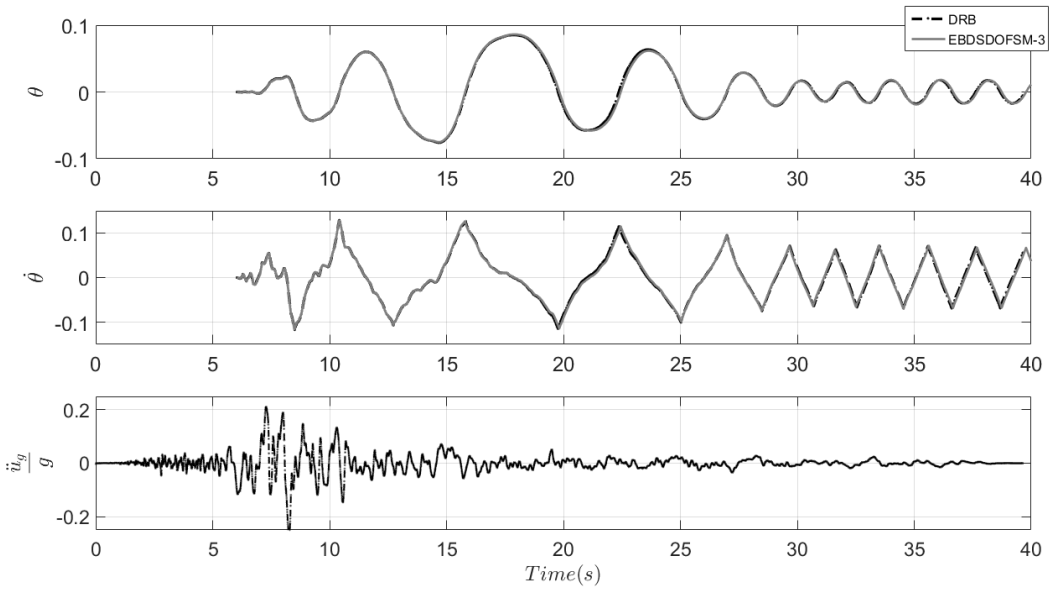

Figure 51: Comparison of rocking rotation and velocity time history response between the DRB and the EBDSDOFSM-3 with R=5m under the Loma Prieta's 1989 earthquake (Station: Hollister Diff Array, φ=165^o, PGA=0.268g).

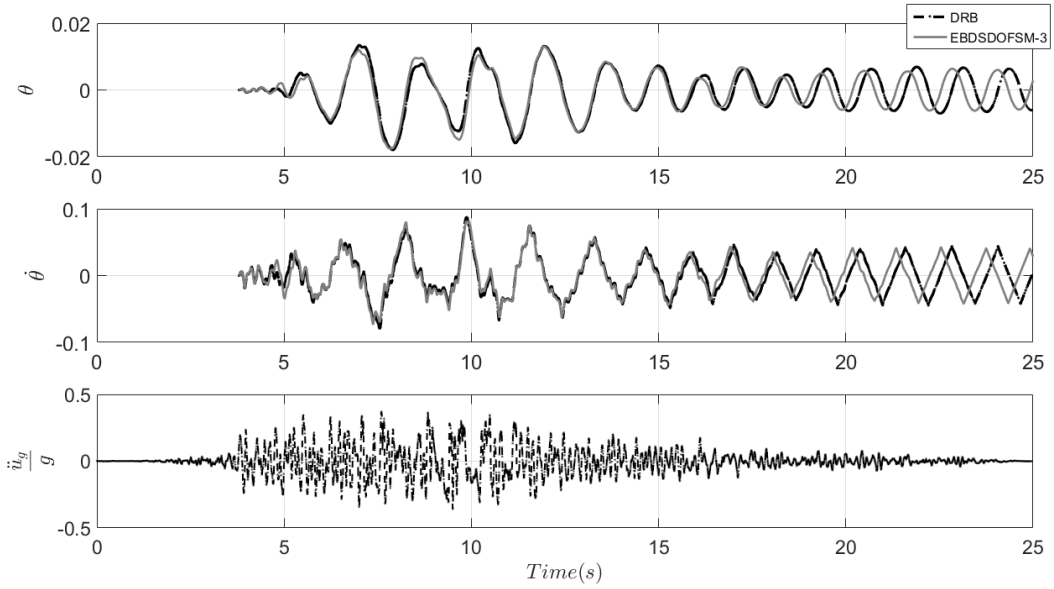

Figure 52: Comparison of rocking rotation and velocity time history response between the DRB and the EBDSDOFSM-3 with R=5m under the Loma Prieta's 1989 earthquake (Station: Waho, φ=0°, PGA=0.37g).

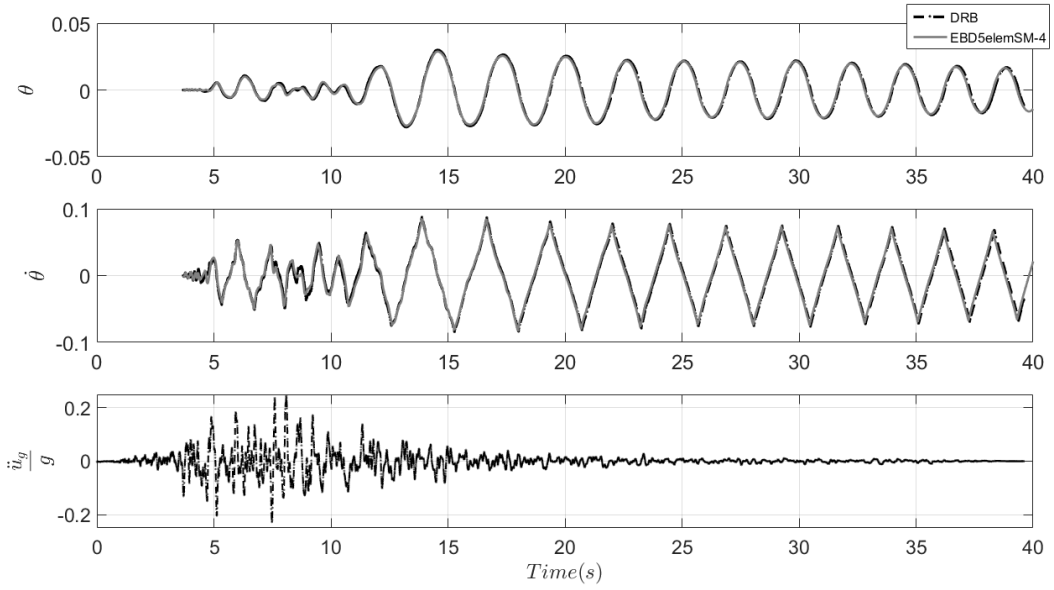

Figure 53: Comparison of rocking rotation and velocity time history response between the DRB and the EBD5elemSM-4 with R=5m under the Loma Prieta's 1989 earthquake (Station: Anderson Dam Downstream, φ=270°, PGA=0.235g).

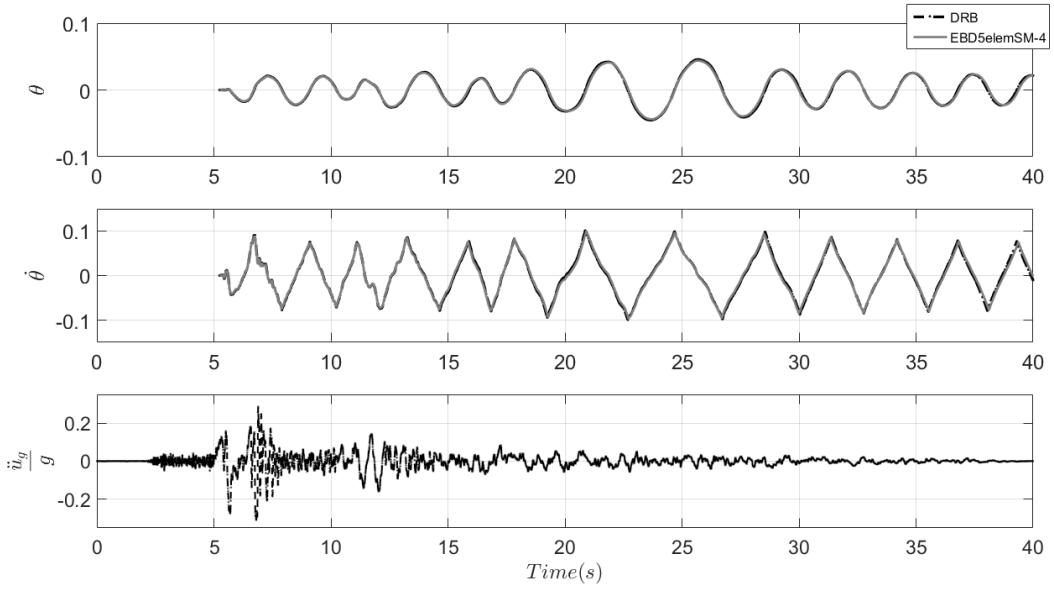

Figure 54: Comparison of rocking rotation and velocity time history response between the DRB and the EBD5elemSM-4 with R=5m under the Imperial Valleys' 1979 earthquake (Station: Cucapah, φ=85°, PGA=0.309g).

- <u>Rocking Blocks with R=2m and slenderness h/b=6.</u>

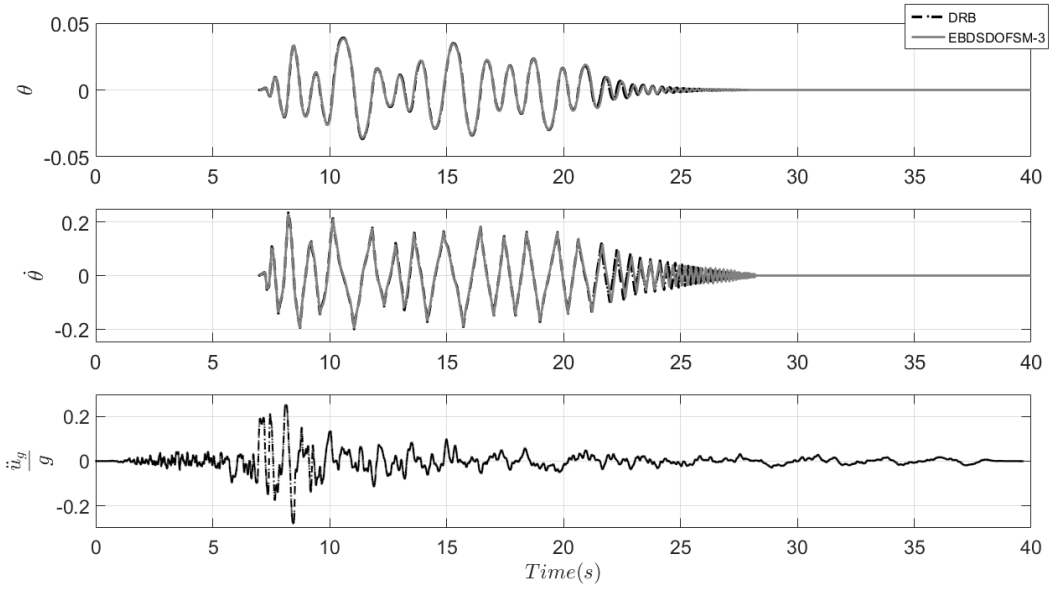

Figure 55: Comparison of rocking rotation and velocity time history response between the DRB and the EBDSDOFSM-3 with R=2m under the Loma Prieta's 1989 earthquake (Station: Hollister Diff Array, φ=255°, PGA=0.279g).

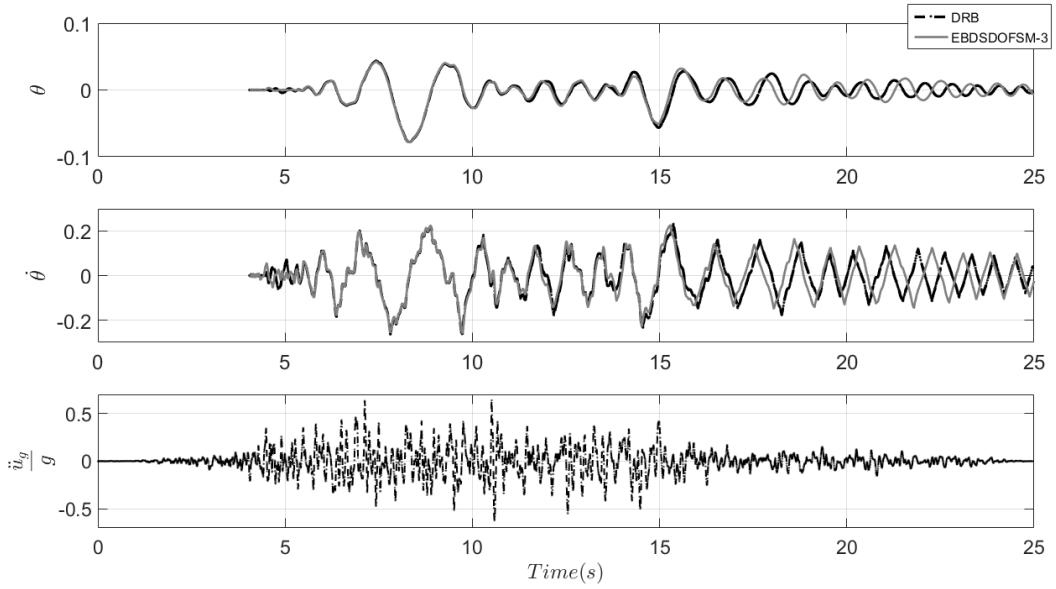

Figure 56: Comparison of rocking rotation and velocity time history response between the DRB and the EBDSDOFSM-3 with R=2m under the Loma Prieta's 1989 earthquake (Station: Waho, φ=90°, PGA=0.638g).

- Rocking Blocks with R=1m and slenderness h/b=6.

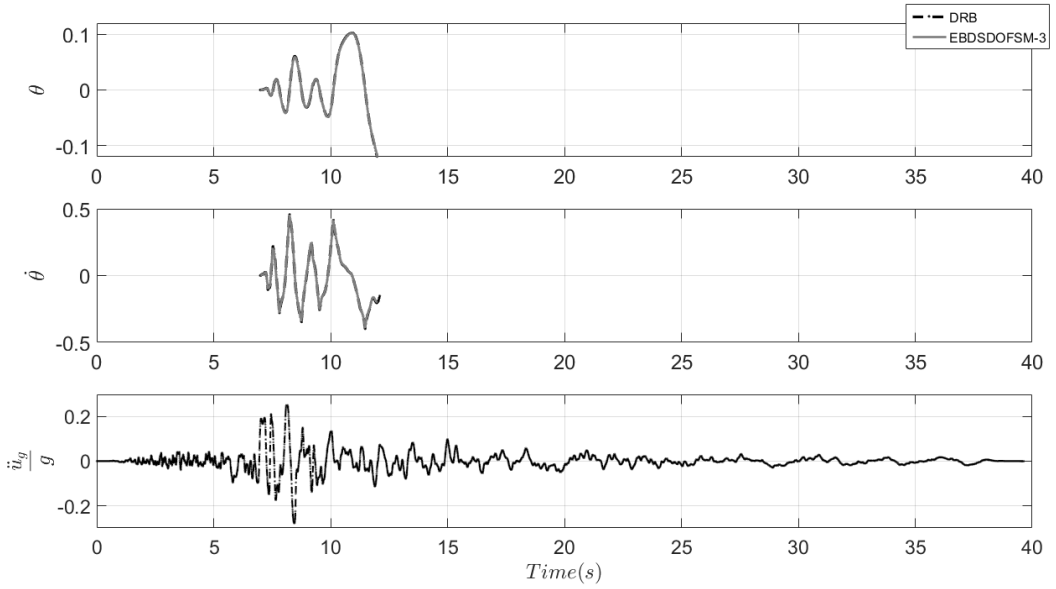

Figure 57: Comparison of rocking rotation and velocity time history response between the DRB and the EBDSDOFSM-3 with R=1m under the Loma Prieta's 1989 earthquake (Station: Hollister Diff Array, φ=255°, PGA=0.279g).

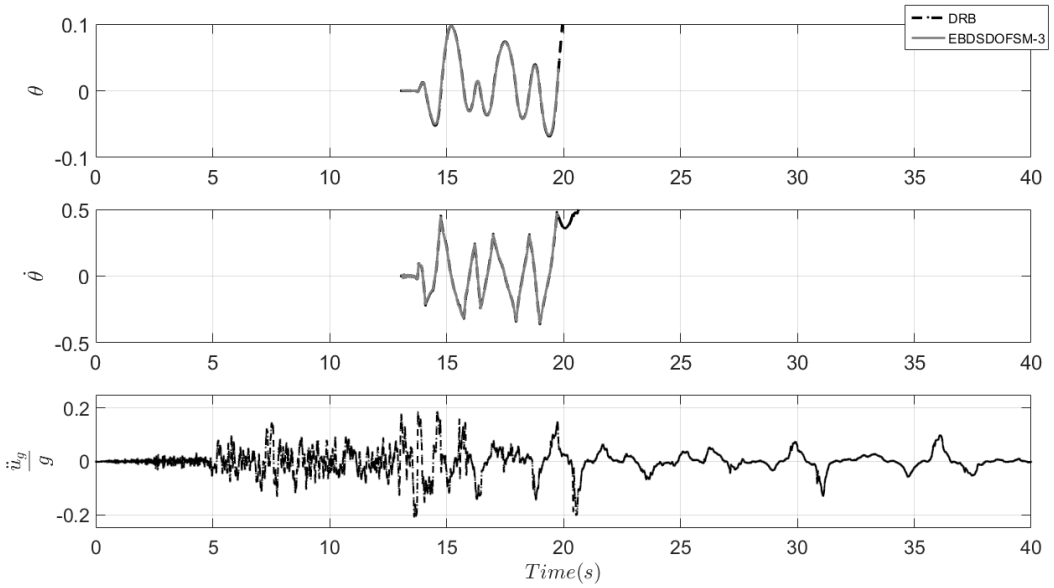

Figure 58: Comparison of rocking rotation and velocity time history response between the DRB and the EBDSDOFSM-3 with R=1m under the Superstition Hills' 1987 earthquake (Station: Wildlife Liquefaction Array, φ=360º, PGA=0.20g).

4. Rocking Response of Damped Flexible Blocks

Relatively few studies have been carried out to investigate the influence of the flexibility of a structure on its rocking behavior taking into account that the rocking response of rigid structures has been studied extensively. In this section is presented an investigation of rocking of flexible blocks and an examination of the limits of the validity of the rigid block assumption that has been used in all the above research. The proposed Spring Model 4 with the event-based damping was extended and modified by assuming that the column represents the rocking body is deformable. For this reason the model was modified by evenly distributing the rotational inertia difference $\Delta I_0 = 4/3mR^2 * (1-\cos^2\alpha)$ among the rotational degrees of freedom of the nodes used to model the column. Namely, a rotational mass equal to ΔI_0 /nnod (where nnod is the number of nodes) is added to the rotational degree of freedom of each node in the finite element model. This means that the column with distributed masses modeled as an Euler-Bernoulli beam-column with a linear elastic material characterized by the elastic modulus E and the density ρ.

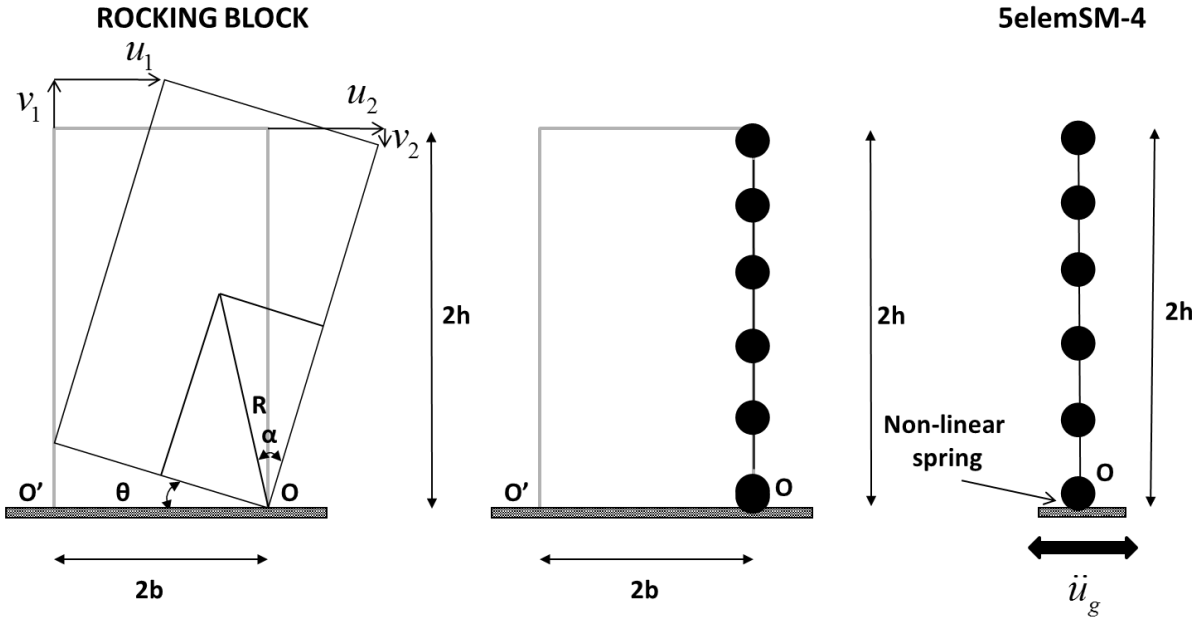

Figure 59: A modified version of 5elemSM-4 suitable to solve flexible blocks

Roh and Reinhorn performed experiments on rocking concrete columns and proved that, for low values of axial force there is no-spalling of concrete when the column uplifts. With this evidence it is assumed that the geometry of the rocking interface does not change and that the column continues to rotate around the pivot points O and O'. As a result, since the vertical reaction at the rocking point (equal to the self-weight of the rocking body) is relatively small, the compression zone of the base cross section tends to become a point.

The overturning instability of a flexible rocking column subjected to a pulse-like ground motion is described by its base rotation and is a function of 7 variables:

$$\theta(t) = f\left(a_p, \omega_p, g, R, \alpha, \zeta, \rho, \mathrm{E}\right) \tag{4.1}$$

Each term of the above equation includes 3 reference dimensions:

$$a_p = \left[LT^{-2}\right], \omega_p = \left[T^{-1}\right], g = \left[LT^{-2}\right], R = \left[L\right], \alpha = [], \zeta = [], \rho = \left[ML^{-3}\right], E = \left[ML^{-1}S^{-2}\right].$$

The damping ratio ζ, is the column first mode flexural vibration damping ratio, modeled in OpenSees using stiffness proportional Rayleigh damping for the nodes of the column, excluding the nodes at the end of the non-linear spring (an option available in OpenSees). Energy dissipation due to rocking is modeled using the event-based damping proposed in the previous chapter. Also, according to Backingham's Π theorem of dimensional analysis the previous equation can be transformed into:

$$\theta(t) = \varphi\left(\frac{a_p}{\tan a}, \frac{\omega_p}{p}, \alpha, \zeta, \frac{E}{\rho g R}\right) \tag{4.2}$$

The departure from the rigid case becomes significant when either E/ρg becomes small or when the column has a large size R. If the material and slenderness α are given, the first eigenperiod of elastic vibration of the flexible solid rectangular column (without rocking) depends only on each size:

$$T_1 = 12.38\sqrt{\frac{\rho}{\mathrm{E}}}\frac{h}{\tan\alpha} \tag{4.3}$$

The flexible rocking bodies are assumed to be made of concrete with E=30GPa and ρ=2.5Mg/m^3. The damping ratio, ζ, of the cantilever was set to 0.01 assuming that the flexible rocking body remains elastic.

Several analyses took place and for the verification of our results arising from the OpenSees model, the block was modeled with a full mesh of quadrilateral elements in the Finite Element software Abaqus.

Two blocks were examined under pulses-like ground excitation and real records. The first block had dimensions 2h=50m and 2b=5m (slenderness tanα=0.1) and the second one had dimensions 2h=25m and 2b=5m (slenderness tanα=0.2).

4.1. Sufficiency of Model-4 in Flexible Bodies

In order to prove that our OpenSees model can extend in deformable rocking bodies, the model examined under a sine pulse and two real records, assuming that there is no damping. The results arising from the comparison of top displacement show that the model can assess the rocking response pretty well. The response of a Flexible Rocking Body (FRB) with dimensions 2h=50m and 2b=5m excited by a sine pulse with T_p=1.6sec and a_p=5gtanα=4.905m/sec^2.

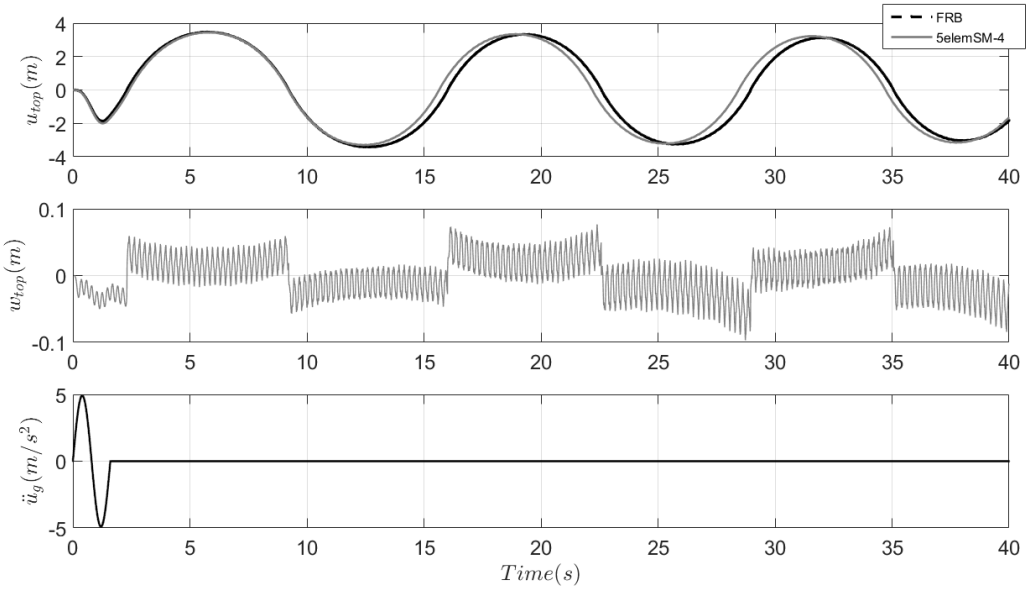

Figure 60: Comparison of top displacement (first row) and top displacement due to bending(second row) time history response between the FRB and the 5elemSM-4 with 2h=50m and tanα=0.1 under a sine pulse with T_p=1.6sec and a_p=5gtanα=4.905m/sec^2.

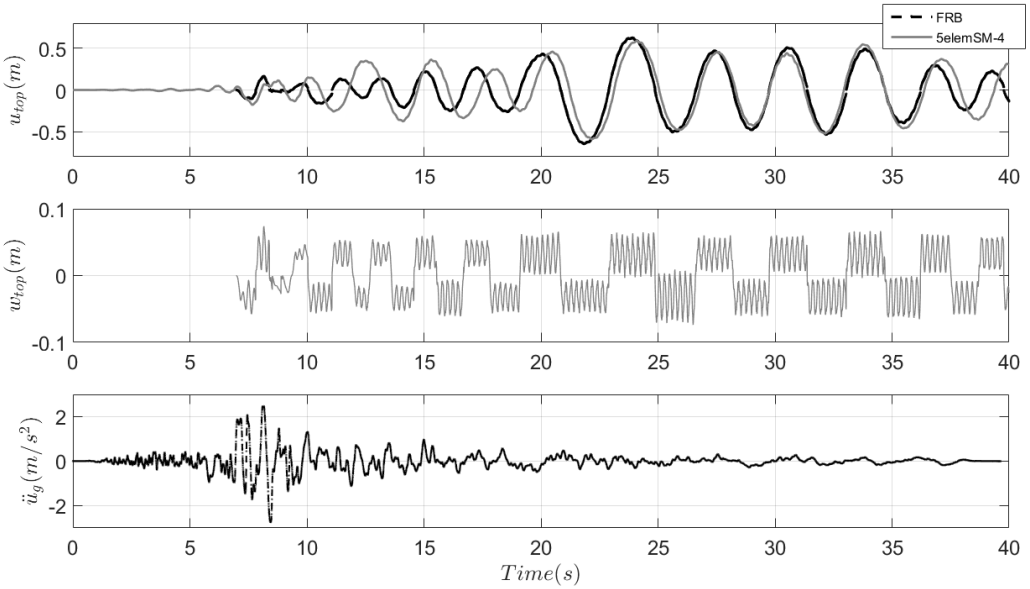

Figure 61: Comparison of top displacement (first row) and top displacement due to bending (second row) time history response between the FRB and the 5elemSM-4 with 2h=50m and tanα=0.1 under the Loma Prieta's 1989 earthquake (Station: Hollister Diff Array, φ=255º, PGA=0.279g).

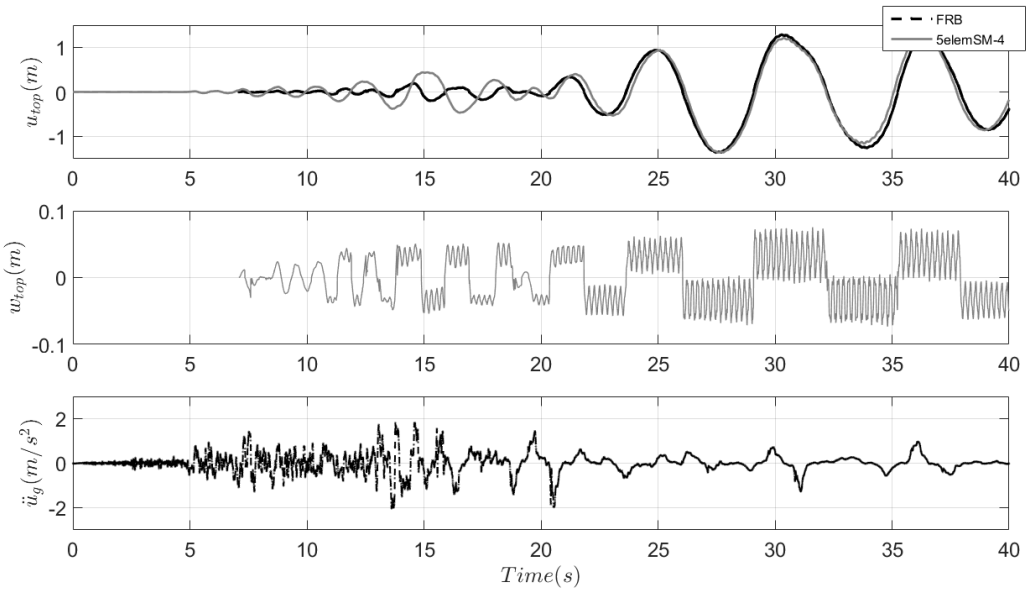

Figure 62: Comparison of top displacement (first row) and top displacement due to bending (second row) time history response between the FRB and the 5elemSM-4 with 2h=50m and tanα=0.1 under the Superstition Hills' 1987 earthquake (Station: Wildlife Liquefaction Array, φ=360º, PGA=0.20g) .

4.2. Parametric Analysis

As it was proved that the model can assess the seismic response under a ground motion, assuming that the coefficient of restitution is acceptable the two blocks of different dimensions are excited and the results included the event-based damping proposed in the previous chapter and the damping ratio, ζ, of Rayleigh damping are presented in the following figures.

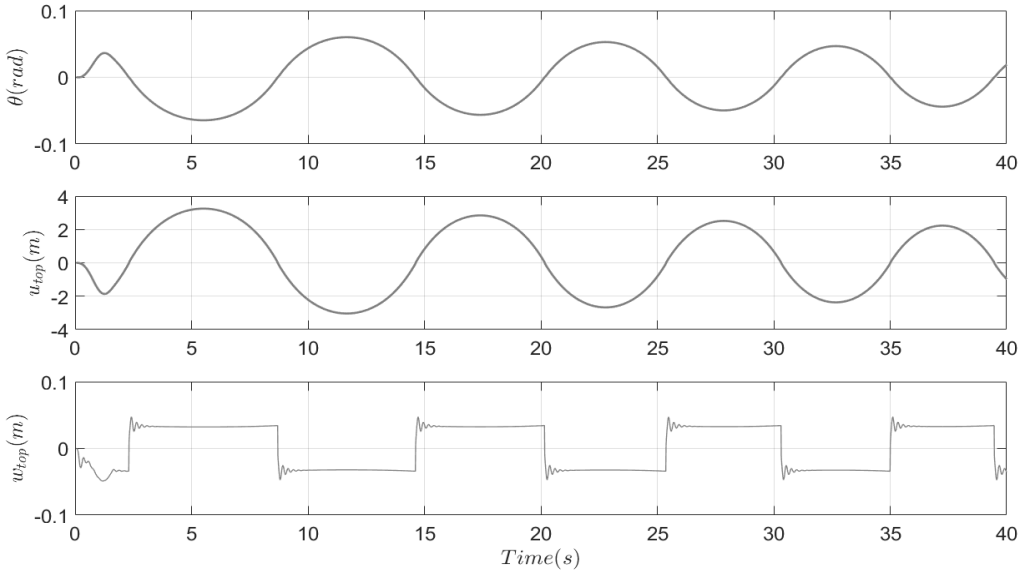

Figure 63: Comparison of rotation(first row), top displacement (second row) and top displacement due to bending (third row) time history response of a damped flexible rocking body with 2h=50m and tanα=0.1 under a sine pulse with T_p=1.6sec and a_p=5gtanα=4.905m/sec^2.

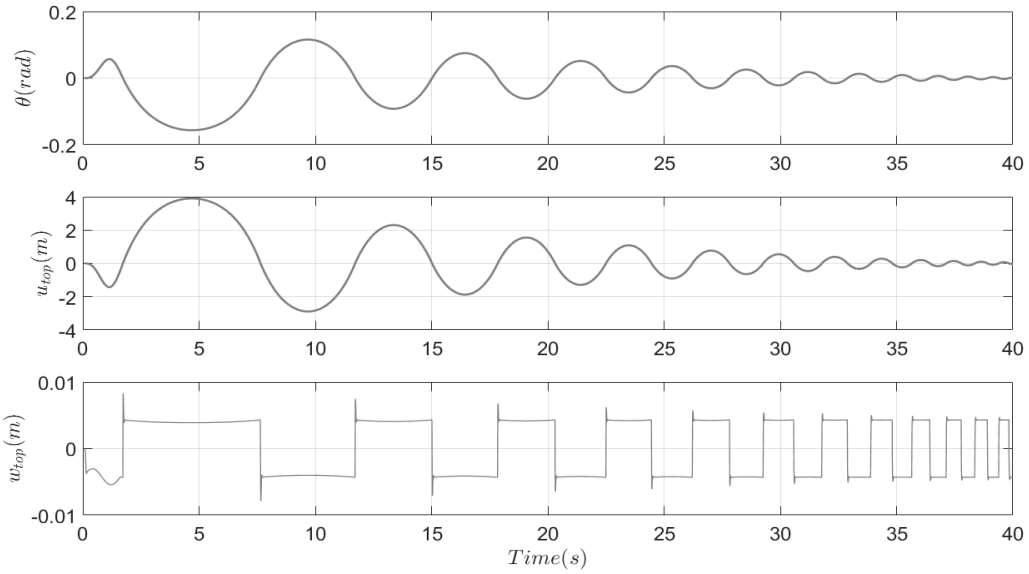

Figure 64: Comparison of rotation(first row), top displacement (second row) and top displacement due to bending (third row) time history response of a damped flexible rocking body with 2h=25m and tanα=0.2 under a sine pulse with T_p=1.6sec and a_p=3gtanα=5.886m/sec^2.

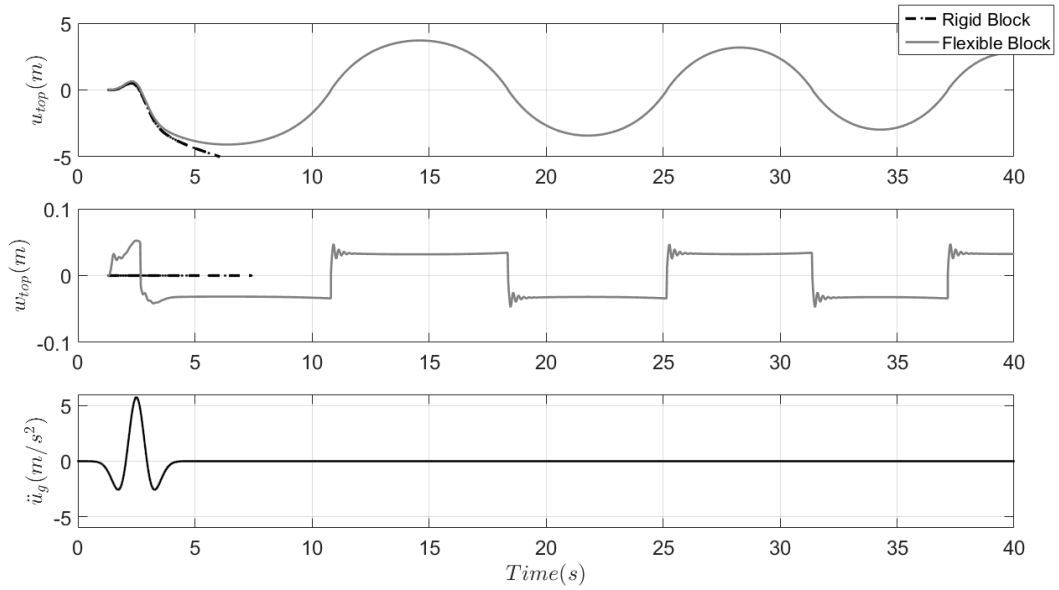

Figure 65: Comparison of top displacement (first row) and top displacement due to bending (second row) time history response of a damped rigid and flexible rocking body with 2h=50m and tanα=0.1 under a Ricker pulse with T_p=2sec and a_p=5.85gtanα=5.74m/sec^2

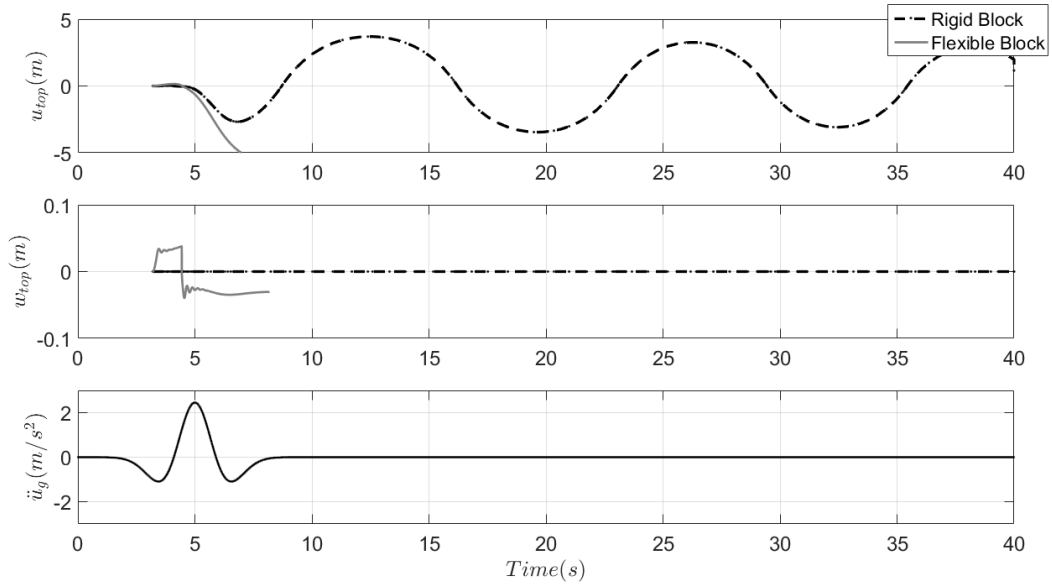

Figure 66: Comparison of top displacement (first row) and top displacement due to bending (second row) time history response of a damped rigid and flexible rocking body with 2h=50m and tanα=0.1 under a Ricker pulse with T_p=4sec and a_p=2.5gtanα=2.45m/sec^2

The above plots indicate that at each rocking impact, the deformation at the top caused by flexure reverses directions. This reversal generates flexural vibration in the column. Hence, part of the rotational kinetic energy of the flexible rocking block is transformed into high frequency flexural vibration energy, which can not cause overturning of the body. This transformation is the reason why the flexible rocking bodies are stable while the rigid rocking body overturns for T_p=2sec. On the other hand, the longer pulse with T_p=4sec has smaller amplitude such that the first part of this pulse only slightly uplifts the rocking body. Then, the flexural vibration caused by the rocking impact is less intense, and most of the kinetic energy is conserved, causing the flexible rocking body to overturn and the rigid rocking body to continue rocking.

5. Concluding Remarks

The purpose of this master's dissertation was the seismic response assessment of rigid and in extension of flexible rocking bodies under an excitation of the base. As it is described in the previous chapters of this dissertation the rocking response of free-standing blocks due to the wide range of nonlinear physical phenomena is a rather difficult task. We have the ability to solve the mathematical formulation if a rigid body rocks on a rigid base. In any other case the response is unpredictable. For this reason in the dissertation we try to solve the rocking problem using the Finite Element Method with Simplified Finite Element Models. The most important investigation was around the energy dissipation and how a Finite Element Model can assess an instantaneous event of energy dissipation at each impact.

Initially, SDOF models are proposed and after a series of analysis we presume that although the difference in the equation of motion and the expected errors the models can approach the response satisfactorily in most cases while the errors are presented in the chapter 2 with comparisons between the displacements, the pushover curves, the moment-rotation relationships and the overturning moments. For slender blocks the results are perfect while for more stocky blocks the errors are more significant. The initial target was the modeling of flexible rocking blocks as the top displacements due to bending change the response and as it is described in the last chapter there are cases that a rigid body is stable and the equivalent flexible overturns and cases that the opposite happens. As a result a fourth model is presented.

On the other hand there is energy dissipation in every impact and a Finite Element Model should be able to approach this dissipation. The first idea, which has been implemented. is a rotational damper in the SM with an equation for the equivalent per-cycle energy loss damping. The rotational damper is able to assess the behavior of the blocks in some cases but further research is needed. Secondly, a numerical damping had been proposed using the Hilber-Huges Algorithm. It works perfectly in the case of pulse-like ground excitation but under real records the results are not likeable. The next step was the simulation of the rocking block as a SDOF with the damping coefficient proposed by FEMA-356. The results are not acceptable in the case of real records.

After all this simulations and inferring that the above ways to approach the damping coefficient are working under some conditions the idea emerged taking into account that the energy dissipation of the rocking block is related with the pre-impact and the post-impact angular velocity. For this reason we correlate the coefficient of restitution, giving the response of a free-standing block, with the velocity of every mass of the models. As a result in each impact the velocity was multiplied with the coefficient of restitution and the new velocities converted to an initial condition in order to continue the analysis. It was proved that the proposed models with the event-based damping and either taking into account the negative stiffness of the block or the large displacements with the corotational formulation the results are very close to the real response of the blocks.

As a summary in this master's dissertation are proposed simplified Finite Element Models able to assess the seismic response of either rigid or flexible rocking bodies and different ways to approach the energy dissipation. The errors are calculated and as a result we can have a full insight for the models. Finally, if the coefficient of restitution is different from the coefficient of restitution proposed by Housner (1963) then the models are able to give the seismic response just by changing this coefficient.

Taking into account the proposed models, the different way to assess the energy dissipation and the extension of the model 4 in flexible systems is proposed for further research the modeling of rocking frames with the Finite Element Method and if experimental results exist a summary comparison between the response of damped flexible bodies and the models aiming to have an equivalent coefficient of restitution.

6. References

1. Housner G.W. (1963). The behavior of inverted pendulum structures during earthquakes. *Bulletin of the Seismological Society of America*, 53(2), 404-417.
2. Vassiliou M.F., Mackie K.R., Stojadinović B. (2014). Dynamic response analysis of solitary flexible rocking bodies: modeling and behavior under pulse-like ground excitation. *Earthquake Engineering and Structural Dynamics*, 43(10), 1463-1481.
3. Yim C.S., Chopra A.K., Penzien J. (1980). Rocking Response of Rigid Blocks to Earthquakes. *Earthquake Engineering and Structural Dynamics*, 8, 565-587.
4. Dimitrakopoulos E.G., Giouvanidis A.I. (2015). Seismic response analysis of the planar rocking frame. *Journal of Engineering Mechanics*, 141(7 04015003).
5. Zhang J., Makris N. (2001). Rocking response of free-standing blocks under cycloidal pulses. *Journal of Engineering Mechanics, ASCE 2001*, 127(5), 473-483.
6. Makris N., Konstantinidis D. (2003). The rocking spectrum and the limitations of practical design methodologies. *Earthquake Engineering and Structural Dynamics*, 32, 265-289.
7. Vassiliou M.F., Mackie K.R., Stojadinović B. (2016). A finite element model for seismic response analysis of deformable rocking frames. *Earthquake Engineering and Structural Dynamics*, 46(3), 447-466.
8. OpenSEES (Open System for Earthquake Engineering Simulations). opensees.berkley.edu
9. MATLAB Version 2015b. The Language of Technical Computing.
10. Dimitrakopoulos E.G., Dejong M.J. (2012). Overturning of Retrofitted Rocking Structures under Pulse-Type Excitations. *Journal of Engineering Mechanics*, 138(8), 963-972.
11. Dejong M.J., Dimitrakopoulos E.G. (2014). Dynamically equivalent rocking structures. *Earthquake Engineering and Structural Dynamics*, 43,1543-1563.
12. Makris N. (2014). The role of the rotational inertia on the seismic resistance of free-standing rocking columns and articulated frames. *Bulletin of the Seismological Society of America*, 104(5), 2226-2239.

13. Chopra A.K., McKenna F. (2016). Modeling viscous damping in nonlinear response history analysis of buildings for earthquake excitation. *Earthquake Engineering and Structural Dynamics,* 45(2), 193-211.
14. Hilber H.M., Hunges T.J., Taylor R.L. (1977). Improved numerical dissipation for time integration algorithms in structural dynamics. *Earthquake Engineering and Structural Dynamics,* 5(3), 283-292.
15. Newmark N.M. (1959). A method of computation of structural dynamics. *Journal of the engineering mechanics division,* 85(3), 67-94.
16. Ricker N. (1943). Further developments in the wavelet theory of seismogram structure. *Bulletin of the Seismological Society of America,* 33, 197-228.
17. Vassiliou M.F., Makris N. (2012). Analysis of the rocking response of rigid blocks standing free on a seismically isolated base. *Earthquake Engineering and Structural Dynamics,* 41(2), 177-196.
18. Vassiliou M.F., Truniger R., Stojadinović B. (2015). An analytical model of a deformable cantilever structure rocking on a rigid surface: development and verification. *Earthquake Engineering and Structural Dynamics* 44(15), 2775-2794.
19. Psycharis I.N., Jennings P.C. (1983). Rocking of slender rigid bodies allowed to uplift. *Earthquake Engineering and Structural Dynamics,* 11, 57-76.
20. Truniger R., Vassiliou M.F., Stojadinović B. (2014). Experimental study of the on the interaction between elasticity and rocking. *Proceedings of the 10th National Conference in Earthquake Engineering,* Earthquake Engineering Research Institute, Anchorage, AK.
21. Konstantinidis D., Makris N. (2010). Experimental and analytical studies of the response of 1/4-scale models of freestanding laboratory equipment subjected to strong earthquake shaking. *Bulletin of Earthquake Engineering, 8(6),* 1457-1477.
22. Psycharis IN. (1983). Dynamics of flexible systems with partial lift-off. *Earthquake Engineering and Structural Dynamics,* 11(4), 501-521.
23. Psycharis IN. (1991). Effect of base uplift on dynamic response of SDOF structures. *Journal of Structural Engineering,* 117(3), 733-754.
24. Spyrakos C.C., Nikolettos G.S. (2005). Overturning stability criteria for fxexible structures to earthquakes. *Journal of Engineering Mechanics*, 131(4), 349-358.

25. FEMA-356 (November 2000). Prestandard and commentary for the seismic rehabilitation of buildings.
26. Pristley MJN, Evison RJ, Carr AJ. (1978). Seismic response of structures free to rock on their foundation. *Bulletin of the New Zealand National Society for Earthquake Engineering*, 11(3), 141-150.
27. Wiebe L. Christopoulos C., Tremblay R., Leclerc M. (2012). Modelling inherent damping for rocking systems: results of large-scale shake table testing. *Proceedings of the 15th World Conference on Earthquake Engineering*, Lisbon, Portugal.
28. ElGawady M.A., Ma Q., Butterrworth J.W., Ingham J. (2011). Effects of interface material on the performance of free rocking blocks. *Earthquake Engineering and Structural Dynamics*, 40, 375-392.
29. Barthes C., Hube M., Stojadinović B. (2010). Dynamics of a Post-Tensioned Rocking Block. *Proceedings of the 9th US National and 10th Canadian Conference on Earthquake Engineering*, Toronto, Canada.
30. Schau H., Johannes M. (2013). Rocking and sliding of unanchored bodies subjected to seismic load according to conventional and nuclear rules. *COMPDYN 2013, 4th ECCOMAS Thematic Conference on Computational Methods in Structural Dynamics and Earthquake Engineering.*
31. Ishiyama Y. (1982). Motions of rigid bodies and criteria for overturning by earthquake excitations. *Earthquake Engineering and Structural Dynamics*, 10, 635-650.
32. Schau H., Johannes M. (2014). Numerical analysis of rocking of unanchored bodies subjected to seismic load using Finite Element analyses. *EURODYN 2014, Proceedings of the 9th International Conference on Structural Dynamics.*
33. Sextos A., Da Porto F., Modena C. (2016). Efficiency of alternative intensity measures for the seismic assessment of monolithic free-standing columns. *Bulleting of Earthquake Engineering.*
34. Dimitrakopoulos E., DeJong M. (2012). Revisiting the rocking block: closed-form solutions similarity laws. *In: Proceedings of Royal Society 468, 2294-2318.*
35. Chatzillari E.T., Tzaros K. (2016). Influence of the friction coefficient in the rocking response of rigid multi-block columns via nonlinear Finite Element analysis. *11th HSTAM International Congress on Mechanics.*

36. ΠΕΤΑΛΑΣ ΑΠΟΣΤΟΛΟΣ (2012). Αριθμητική διερεύνηση της λικνιστικής απόκρισης συμπαγών σωμάτων. *Διπλωματική εργασία, Αριστοτέλειο Πανεπιστήμιο Θεσσαλονίκης.*
37. ΟΛΥΜΠΙΑ ΤΑΣΚΑΡΗ (με τη συνδρομή των: ΛΕΥΤΕΡΗ ΤΣΑΚΜΑΚΙΔΗ και ΚΩΣΤΑ ΚΑΤΑΚΑΛΟΥ). Abaqus/CAE Version 6.4 Tutorial. *Αριστοτέλειο Πανεπιστήμιο Θεσσαλονίκης.*